

***B* Flavour Anomalies: 2021 Theoretical Status Report¹**

David London ^{a,2} and Joaquim Matias ^{b,c,3}

*a: Physique des Particules, Université de Montréal,
1375 Avenue Thérèse-Lavoie-Roux, Montréal, QC, Canada H2V 0B3*
*b: Universitat Autònoma de Barcelona,
E-08193 Bellaterra (Barcelona), Spain*
*c: Institut de Física d'Altes Energies and
The Barcelona Institute of Science and Technology, Spain*

(November 18, 2021)

Abstract

At the present time, there are discrepancies with the predictions of the SM in several observables involving $b \rightarrow s\ell^+\ell^-$ and $b \rightarrow c\ell^-\bar{\nu}_\ell$ decays. These are the B flavour anomalies. In this review, we summarize the data as of Moriond 2021 and present theoretical new-physics explanations from both a model-independent effective-field-theory point of view and through the building of explicit models. Throughout, we stress the complementarity of these two approaches. We also discuss combined explanations of both B anomalies, and present models that also explain other problems, such as dark matter, $(g-2)_\mu$, neutrino properties, and hadronic anomalies.

¹To be published in the *Annual Review of Nuclear and Particle Science*

²london@lps.umontreal.ca

³matias@ifae.es

1 Introduction

At the present time (2021), there are a number of measurements of observables involving B -meson decays that are in disagreement with the predictions of the standard model (SM). These are the B flavour anomalies. There are two types. The neutral-current anomalies are found in processes involving $b \rightarrow s\ell^+\ell^-$ decays, while the charged-current anomalies involve $b \rightarrow c\ell^-\bar{\nu}_\ell$.

The first observation of the $b \rightarrow s\ell^+\ell^-$ anomaly was in 2013. At the EPS conference in Stockholm, the LHCb Collaboration announced [1] that they had measured the observable P'_5 [2] in the four-body angular distribution $B_d \rightarrow K^{*0}(\rightarrow K^+\pi^-)\mu^+\mu^-$, and found that it disagreed with the SM prediction at the level of 3.7σ [3]. Soon thereafter, another, smaller discrepancy of 2.6σ was found in the measurement of $R_K \equiv \mathcal{B}(B^+ \rightarrow K^+\mu^+\mu^-)/\mathcal{B}(B^+ \rightarrow K^+e^+e^-)$ [4]. The SM predicts $R_K \simeq 1$ [5], so the experimental result suggests the violation of lepton flavour universality, i.e., the violation of the property that the interactions between gauge bosons and charged leptons are the same for all generations of leptons. Since then, the number of measured observables involving $b \rightarrow s\ell^+\ell^-$ decays has grown enormously, and many of these also exhibit discrepancies with the SM. What is particularly striking here is the consistency of these measurements: the discrepancies all go in the same direction, pointing to a common new-physics explanation.

The first measurement of a $b \rightarrow c\ell^-\bar{\nu}_\ell$ anomaly was in 2012: the BaBar Collaboration measured $R_{D^{(*)}} \equiv \mathcal{B}(\bar{B} \rightarrow D^{(*)}\tau^-\bar{\nu}_\tau)/\mathcal{B}(\bar{B} \rightarrow D^{(*)}\ell^-\bar{\nu}_\ell)$ ($\ell = e, \mu$), and found values for R_D and R_{D^*} that, when taken together, exceed the SM expectation by 3.4σ [6]. These measurements were repeated by BaBar (2013) [7], Belle (2015) [8] and LHCb (2015) [9], and the results were largely confirmed. Here too, measurements of additional $b \rightarrow c\ell^-\bar{\nu}_\ell$ observables have been made subsequently (though far fewer than in the $b \rightarrow s\ell^+\ell^-$ case), and other deviations from the SM predictions have been found.

Now, the SM has made a great number of predictions, most of which have been confirmed (e.g., the discovery of the Higgs boson). However, it also leaves many questions unanswered (what is dark matter?, what is the origin of the baryon asymmetry of the universe? why are there three generations?, etc.). For this reason, it is clear that the SM is not complete – there must be physics beyond the SM. The B flavour anomalies have been around for almost ten years. They have been observed in a variety of processes, and by different experiments. We may in fact be seeing the first signs of new physics. For this reason, the study of the B flavour anomalies has become a very exciting subject. A great deal of work has been done, by many people, with the aim of finding explanations of the $b \rightarrow s\ell^+\ell^-$ and $b \rightarrow c\ell^-\bar{\nu}_\ell$ anomalies, either individually or simultaneously.

In this review we present a status report on the B flavour anomalies from a theoretical perspective. For each of the $b \rightarrow s\ell^+\ell^-$ and $b \rightarrow c\ell^-\bar{\nu}_\ell$ anomalies, we examine possible solutions from an effective-field-theory point of view (global analyses), and in the context of model building. Throughout, we stress the complementarity of these two approaches. We also review the combined explanations of the two types of anomalies, as well as models that attempt to also explain other discrepancies with the SM (dark matter, $(g-2)_\mu$, etc.). Finally, we take a glance into the future, pointing out interesting observables whose

measurement can distinguish various explanations.

Notation: The material in this review is taken from many different sources, which have different notations. We have tried to uniformize this notation as follows. In currents, Q and L represent left-handed (LH) $SU(2)_L$ quark and lepton doublets, respectively, of any generation. Similarly, u , d and e represent right-handed (RH) $SU(2)_L$ -singlet up-type quarks, down-type quarks and charged leptons, respectively, of any generation. For all of these fields, the chirality is not explicitly indicated. The symbols b , s , c , μ , τ and ν_τ refer to the actual particles. If it is necessary to specify the chirality of the b , we write $b_{L,R}$ or $P_{L,R}b$, where $P_{L,R} = (1 \mp \gamma_5)/2$ are the LH and RH projection operators, and similarly for the other particles. Finally, ℓ stands for e , μ or τ , unless otherwise indicated.

2 EFTs and model building: two complementary approaches

The B anomalies suggest the presence of physics beyond the SM. The next question is then: what can this new physics (NP) be? There are two different ways of addressing this question. The first uses a model-independent effective-field-theory (EFT) approach: an effective Hamiltonian is written that contains all dimension-6 operators that describe the decay of interest ($b \rightarrow s\ell^+\ell^-$ or $b \rightarrow c\ell^-\bar{\nu}_\ell$). A global fit to all the data is performed to find the preferred values of the coefficients of these operators (the Wilson coefficients (WCs)). The second approach is to construct models of NP that reproduce the data. Both methods have their advantages and disadvantages; by combining the two, one can get a complete idea of possible NP solutions.

The exchange of NP particles generates new interactions among the SM particles, in particular the $b \rightarrow s\ell^+\ell^-$ or $b \rightarrow c\ell^-\bar{\nu}_\ell$ four-fermion operators. Now, to date, no new particles have been observed at the LHC. As a consequence, it is generally believed that the NP, whatever it is, must be heavy, with masses of $\mathcal{O}(\text{TeV})$. This is above the electroweak scale, so that, when the NP particles are integrated out, the EFT produced is invariant under the full SM gauge group, $SU(3)_C \times SU(2)_L \times U(1)_Y$. This is the SM effective field theory (SMEFT). In it, all dimension-4 operators are those of the SM; higher-dimension operators are due to NP. These additional operators are suppressed by powers of Λ , the scale of NP. It is the SMEFT that provides the connection between the two approaches.

The operators in the SMEFT are independent. However, a particular model will generate only a subset of all SMEFT operators, and the coefficients of these operators will often be related. This means that a model analysis must take into account additional constraints, not just those of the B anomalies.

While the SMEFT applies to TeV-scale physics, the EFT used in the global fits is appropriate for physics at the scale m_b . That is, it is invariant under $SU(3)_C \times U(1)_{em}$ and all particles with masses greater than m_b have been integrated out. This is the WET (weak effective theory).

Since they apply to lower-energy physics, all WET operators can be mapped to SMEFT operators. This has several consequences. First, those WET dimension-6 operators that also obey $SU(3)_C \times SU(2)_L \times U(1)_Y$ are related to (combinations of) dimension-6 SMEFT

operators. But those WET operators that do not respect this symmetry are mapped at tree level to higher-dimensional SMEFT operators, typically dimension 8. These dimension-8 operators involve additional Higgs fields, and the WET operators are generated when the Higgs gets a vev v . Thus, the WET operators are suppressed by an additional factor of v^2/Λ^2 , and can be neglected.

Another effect, more related to model building, is the following. EFT analyses often use a basis for the dimension-6 WET operators that is not the same as that of SMEFT. That is, a dimension-6 WET operator may be mapped to a linear combination of dimension-6 SMEFT operators. However, within the SMEFT, these operators are a-priori independent. Thus, if the EFT analysis favours NP in a WET operator that is a combination of SMEFT operators, this indicates that there must be an additional symmetry relating these operators. This is a clue for the model builders. (And if such a symmetry does not seem to exist, or is very contrived, then perhaps this EFT scenario will be disfavoured in spite of the good fit.)

Indeed, using EFT global-fit analyses, a variety of scenarios have been proposed in which the NP contributes to different WCs. For several of these scenarios, models can be constructed with the help of the SMEFT. In addition, by looking at SMEFT operators, one sees that a simultaneous explanation of both $b \rightarrow s\ell^+\ell^-$ and $b \rightarrow c\ell^-\bar{\nu}_\ell$ anomalies is possible.

The bottom line is that the EFT and model-building approaches are complementary, and the addition of SMEFT information provides a complete overview of possible NP explanations of the B flavour anomalies.

3 Neutral-current anomalies: $b \rightarrow s\ell^+\ell^-$

We begin by examining the neutral-current B flavour anomalies observed in $b \rightarrow s\ell^+\ell^-$ transitions. In the SM, this decay occurs at the one-loop level.

3.1 $b \rightarrow s\ell^+\ell^-$ observables

There are two different categories of $b \rightarrow s\ell^+\ell^-$ observables that exhibit tension with the predictions of the SM:

1. Observables involving only the $b \rightarrow s\mu^+\mu^-$ transition. Here there are two types that differ in their sensitivity to hadronic uncertainties and NP:
 - Branching ratios include $\mathcal{B}(B^0 \rightarrow K^{0*}\mu^+\mu^-)$, $\mathcal{B}(B^+ \rightarrow K^{*+}\mu^+\mu^-)$, $\mathcal{B}(B_s \rightarrow \phi\mu^+\mu^-)$, $\mathcal{B}(B^+ \rightarrow K^+\mu^+\mu^-)$ and $\mathcal{B}(B^0 \rightarrow K^0\mu^+\mu^-)$.
 - Observables that parametrize the four-body angular distribution $B \rightarrow K^*(\rightarrow K\pi)\mu^+\mu^-$ or $B_s \rightarrow \phi(\rightarrow K^+K^-)\mu^+\mu^-$. These distributions are functions of the three angles that characterize the final four-particle state and q^2 , the dilepton invariant mass-squared (see Ref. [10]). The q^2 spectrum can be split into three regions: (i) large K^* recoil, $4m_\ell^2 \leq q^2 \leq 9 \text{ GeV}^2$: here, $E_{K^*} \gg \Lambda_{QCD}$, this

includes the region near the photon pole, (ii) charmonium region, $9 < q^2 < 14$ GeV²: this includes the charmonium resonances (J/ψ , etc.), (iii) low K^* recoil, $14 < q^2 < (m_B - m_{K^*})^2$ GeV²: here, $E_{K^*} \simeq \Lambda_{QCD}$. Each region requires a different treatment of hadronic uncertainties.

The angular observables can be further separated into two categories, differentiated by their sensitivity to hadronic effects. The non-optimized observables (the S_i [11]) are more sensitive to hadronic uncertainties, while the optimized observables (the P_i [10, 13, 14])⁴ are constructed so that the dependence on soft form factors cancels exactly at leading order. They are usually measured in q^2 bins.

2. Observables that measure lepton-flavour-universality violation (LFUV). The gauge bosons of the SM couple identically (i.e., universally) to charged leptons of different generations. The LFUV observables include

$$R_K = \frac{\mathcal{B}(B^+ \rightarrow K^+ \mu^+ \mu^-)}{\mathcal{B}(B^+ \rightarrow K^+ e^+ e^-)}, \quad R_{K^*} = \frac{\mathcal{B}(B \rightarrow K^* \mu^+ \mu^-)}{\mathcal{B}(B \rightarrow K^* e^+ e^-)},$$

$$R_\phi = \frac{\mathcal{B}(B_s \rightarrow \phi \mu^+ \mu^-)}{\mathcal{B}(B_s \rightarrow \phi e^+ e^-)}. \quad (1)$$

The SM predicts that all of these ratios equal 1 (up to tiny lepton mass and electromagnetic effects, see Refs. [16, 17]). A deviation from this prediction in the measurement of any of these observables would signal the breaking of lepton-flavour universality. R_K and R_{K^*} have been measured by LHCb [18, 19] and Belle [20, 21]. Additional LFUV observables can be constructed using optimized observables [22]:

$$Q_i = P_i^{\mu} - P_i^e \quad (2)$$

The SM predicts them to vanish to high accuracy. Two of these – $Q_{4,5}$ – have already been measured by Belle [23].

Three other types of observables are usually included in the global fits. (i) There are inclusive decays such as $B \rightarrow X_s \mu^+ \mu^-$ (these measurements are still not very precise). (ii) $\mathcal{B}(B_s \rightarrow \mu^+ \mu^-)$ has been measured by LHCb, ATLAS and CMS. This observable is particularly interesting due to its reduced hadronic sensitivity and its dependence on a reduced subset of Wilson coefficients (see next section). The discrepancy of this measurement with the SM is at the level of $\sim 2\sigma$. (iii) There are radiative observables such as $B \rightarrow X_s \gamma$, $B_s \rightarrow \phi \gamma$ and $B \rightarrow K^* \gamma$. Further details on the experimental status of all of these observables can be found in Ref. [24].

⁴The first optimized observable, A_T^i , was introduced in Ref. [10], followed some years later by two additional transverse asymmetries in Ref. [12]. A complete basis to describe the four-body angular distribution was introduced afterwards in Ref. [13], and it was redefined in Ref. [14] to adapt more easily to the experimental measurements. A generalization of the angular-distribution formalism can be found in Ref. [15].

3.2 EFT analysis

3.2.1 Operators

In the most general case, $b \rightarrow s\ell^+\ell^-$ transitions are described by an effective Hamiltonian [25]⁵

$$\mathcal{H}_{\text{eff}} = -\frac{4G_F}{\sqrt{2}} V_{tb}V_{ts}^* \frac{e^2}{16\pi^2} \sum_{i=1}^{12} C_i \mathcal{O}_i , \quad (3)$$

where V_{ij} are elements of the Cabibbo-Kobayashi-Maskawa (CKM) matrix, and the operators are⁶

$$\begin{aligned} \mathcal{O}_7^{(\prime)} &= \frac{m_b}{e} (\bar{s}\sigma_{\mu\nu}P_{R(L)}b)F^{\mu\nu} , \\ \mathcal{O}_{9\ell}^{(\prime)} &= (\bar{s}\gamma_\mu P_{L(R)}b)(\bar{\ell}\gamma^\mu\ell) \quad , \quad \mathcal{O}_{10\ell}^{(\prime)} = (\bar{s}\gamma_\mu P_{L(R)}b)(\bar{\ell}\gamma^\mu\gamma_5\ell) , \\ \mathcal{O}_{S\ell}^{(\prime)} &= (\bar{s}P_{R(L)}b)(\bar{\ell}\ell) \quad , \quad \mathcal{O}_{P\ell}^{(\prime)} = (\bar{s}P_{R(L)}b)(\bar{\ell}\gamma_5\ell) , \\ \mathcal{O}_{T\ell} &= (\bar{s}\sigma_{\mu\nu}b)(\bar{\ell}\sigma^{\mu\nu}\ell) \quad , \quad \mathcal{O}_{T5\ell} = (\bar{s}\sigma_{\mu\nu}b)(\bar{\ell}\sigma^{\mu\nu}\gamma_5\ell) . \end{aligned} \quad (4)$$

With \mathcal{H}_{eff} , the short- and long-distance physics are separated: all the information about the heavy degrees of freedom that have been integrated out (both SM and NP particles) is encoded in the Wilson coefficients of the operators, C_i .

It is useful to relate these operators to those of the SMEFT. To this end, we take linear combinations of them to form operators involving only LH and RH fermions:

$$\begin{aligned} \mathcal{O}_{V\ell}^{ij} &= (\bar{s}\gamma_\mu P_i b)(\bar{\ell}\gamma^\mu P_j \ell) \quad , \quad \mathcal{O}_{S\ell}^{ij} = (\bar{s}P_i b)(\bar{\ell}P_j \ell) \quad , \\ \mathcal{O}_{T\ell}^i &= (\bar{s}\sigma_{\mu\nu} P_i b)(\bar{\ell}\sigma^{\mu\nu} P_i \ell) \quad , \quad i, j = L, R . \end{aligned} \quad (5)$$

Of these ten WET operators, four of them – $\mathcal{O}_{S\ell}^{LL}$, $\mathcal{O}_{S\ell}^{RR}$, $\mathcal{O}_{T\ell}^L$ and $\mathcal{O}_{T\ell}^R$ – are not generated at dimension 6 in SMEFT [26]; in fact, they are generated at dimension 8 [137]. They are therefore suppressed by v^2/Λ^2 compared to the other six operators, and can be neglected. The two remaining scalar operators are often written in the literature as

$$\mathcal{O}_{S\ell}^{(\prime)} = (\bar{s}P_{R(L)}b)(\bar{\ell}\ell) \quad , \quad \mathcal{O}_{P\ell}^{(\prime)} = (\bar{s}P_{R(L)}b)(\bar{\ell}\gamma_5\ell) , \quad (6)$$

with conditions imposed on the WCs: $C_{S\ell} = -C_{P\ell}$ and $C'_{S\ell} = C'_{P\ell}$ [26].

\mathcal{H}_{eff} therefore contains eight operators describing $b \rightarrow s\ell^+\ell^-$ transitions. The SM contributes mainly to the WCs of three of these: \mathcal{O}_7 , $\mathcal{O}_{9\ell}$ and $\mathcal{O}_{10\ell}$ (there is also a tiny contribution to C'_7). The values of their coefficients at the scale $\mu = 4.8$ GeV are [27, 28, 29, 30, 31]

$$C_7^{\text{SM}}(\mu_b) = -0.29 \quad , \quad C_9^{\text{effSM}}(\mu_b) = 4.1 \quad , \quad C_{10}^{\text{SM}}(\mu_b) = -4.3 . \quad (7)$$

⁵This operator basis was chosen in Ref. [25] because it is useful to describe the SM contributions to $b \rightarrow s\ell^+\ell^-$. Historically, this basis has also been used to describe the NP contributions. However, other choices of basis are equivalent and equally valid.

⁶Note that, in the literature, the scalar and pseudoscalar operators are sometimes multiplied by m_b .

NP can contribute to all eight operators. The WCs encode the short-distance physics and contain both SM and NP information: $\mathcal{C}_i = \mathcal{C}_i^{\text{SM}} + \mathcal{C}_i^{\text{NP}}$. All of these operators (or subsets of them) enter the observables discussed above. For instance, the angular and LFUV observables receive contributions from all operators (or combinations of them), radiative observables probe the electromagnetic operators $\mathcal{O}_7^{(\prime)}$, and $\mathcal{B}_{B_s \rightarrow \mu^+ \mu^-}$ is sensitive to the scalar and vector-axial operators.

3.2.2 Methodology

In Sec. 3.1, we presented the list of $b \rightarrow s\ell^+\ell^-$ observables, some of which exhibit deviations from the predictions of the SM. In order to determine whether these form a coherent set of deviations that have a common explanation, it is necessary to perform a global fit of all observables. There are two approaches to performing such a statistical analysis, the frequentist and the Bayesian methods. The frequentist approach is most commonly used to analyze the $b \rightarrow s\ell^+\ell^-$ anomalies, and this is what we focus on in this review. (See Refs. [32, 33, 34] for Bayesian analyses.)

Global fits have been performed by a number of groups, but there are three in particular that have provided regular updates⁷. We refer to these groups as ACDMN (Algueró/Capdevila/Descotes-Genon/Matias/Novoa-Brunet) [37, 38, 49], AS (Altmannshofer/Stangl) [50] and HMMN (Hurth/Mahmoudi/Martinez Santos/Neshatpour) [52]. (These names appear on the latest update; for all three groups, other authors have been involved over the years.) In this review, we compare the methodologies and results of all three groups, but we occasionally focus a bit more on the results of ACDMN. In performing a fit, it is necessary to choose a basis for the $b \rightarrow s\ell^+\ell^-$ operators, and the basis of Eq. (4) is usually used. (However, when the results are compared with the SMEFT, it will be useful to take linear combinations of these operators.)

The analysis of ACDMN is done using a likelihood approach to fit the deviations from the SM values of the relevant WCs, taking into account the experimental and theoretical uncertainties as well as their correlations in Gaussian approximation. The main differences in the set-ups of the global fits of ACDMN, AS and HMMN are:

- Number of observables. There are two types of fits: (i) a complete fit, including all observables, and (ii) a fit including only the LFUV observables. For ACDMN, the complete fit includes all available data (with one important exception, discussed below), for a total of 246 observables (from LHCb, ATLAS, CMS and Belle). The LFUV fit includes $R_{K,K^*}, Q_{4,5}$ and the radiative decays. In contrast, for their complete fit, AS uses only a subset of the available data, with a total of 130 observables [51]. But for their LFUV fit, they use the same observables as ACDMN. Finally, the complete fit of HMMN is reasonably exhaustive, including 173 observables. But the Q_i are left out of the LFUV fit in HMMN.

The one process whose observables are excluded from the analysis of ACDMN, but is included in that of AS and HMMN, is the baryonic decay $\Lambda_b \rightarrow \Lambda \mu^+ \mu^-$. The rea-

⁷Other recent global fits can be found in Refs. [35, 36].

son for its exclusion is as follows. The normalization of $\mathcal{B}(\Lambda_b \rightarrow \Lambda \mu^+ \mu^-)$ was taken by LHCb from LEP and Tevatron, and required a correct scaling of the ratio of productions between LHC, LEP and Tevatron. However, while the branching ratio is provided in bins at LHCb, it was never measured in bins at Tevatron. Furthermore, combining LEP and Tevatron data is delicate, given the strong dependence on the b -quark production process. Thus, the ratio of productions depends also on the kinematics, so that taking this input from LEP and Tevatron introduces some uncertainty and model dependence in the normalization [33, 39].

- Wilson coefficients included in the global fits. The $b \rightarrow s \ell^+ \ell^-$ operators that can receive NP contributions can be separated into three types: electromagnetic ($\mathcal{O}_7^{(\prime)}$, Eq. (4)), vector/axial vector ($\mathcal{O}_{9\ell}^{(\prime)}$ and $\mathcal{O}_{10\ell}^{(\prime)}$, Eq. (4)), and scalar/pseudoscalar ($\mathcal{O}_{S\ell}^{(\prime)}$ and $\mathcal{O}_{P\ell}^{(\prime)}$, Eq. (6)). In ACDMN's analysis, all electromagnetic and vector/axial vector operators are included, but not scalar/pseudoscalar operators. In the analysis of AS, the vector/axial vector and scalar/pseudoscalar operators are included, but not electromagnetic operators. And HMMN include all operators.
- Treatment of the covariance matrix. ACDMN use the covariance matrix in the SM after checking in different points of the NP parameter space that the variation of the covariance matrix is not significant. On the other hand, AS compute a covariance matrix at each point. This is exact for branching ratios which are second-order polynomials in the WCs, but for the angular observables and LFUV ratios it is done approximately by expanding the numerator and denominator up to second-order polynomials, assuming small NP contributions to the WCs compared to the SM. The range of validity of this approximation is roughly the same as taking the SM covariance matrix everywhere.

3.2.3 Hadronic uncertainties

The impact of hadronic uncertainties on the observables of the B anomalies has been object of very intense debates in the past (for a complete discussion, see Refs. [40, 41]). However, important progress on these uncertainties from explicit computations has been made recently, and this has clarified the situation.

There are two main sources of hadronic uncertainties affecting exclusive B decays. The first is form factors (FFs). These are local contributions that parametrize the transition of a B meson to a final-state meson M . In our case, we are interested in the FFs for $B \rightarrow K^{(*)}$ and $B_s \rightarrow \phi$. The second is non-local contributions associated with charm-quark loops. In what follows, we denote these as T_μ .

The amplitude for the decay $B \rightarrow M \ell^+ \ell^-$ has the following structure in the SM:

$$A(B \rightarrow M \ell^+ \ell^-) = \frac{G_F \alpha}{\sqrt{2} \pi} V_{tb} V_{ts}^* [(A_\mu + T_\mu) \bar{u}_\ell \gamma^\mu v_\ell + B_\mu \bar{u}_\ell \gamma^\mu \gamma_5 v_\ell], \quad (8)$$

where $A_\mu = -(2m_b q^\nu / q^2) \mathcal{C}_7 \langle M | \bar{s} \sigma_{\mu\nu} P_R b | B \rangle + \mathcal{C}_9 \langle M | \bar{s} \gamma_\mu P_L b | B \rangle$ and $B_\mu = \mathcal{C}_{10} \langle M | \bar{s} \gamma_\mu P_L b | B \rangle$. The local contributions from FFs are included in A_μ and B_μ . At low q^2 , these FFs are

computed using light-cone sum rules (LCSR) with B -meson [42] or light-meson distribution amplitudes (DAs) [44]. Recently, important updates that include higher-twist effects in the B -meson DA have been presented in the literature [43]. At high q^2 , FFs are taken mainly from lattice computations. In addition, it is customary to extrapolate the lattice computations to low q^2 in order to reduce the uncertainty of the LCSR low- q^2 computation. The analysis of ACDMN is done using the B -meson DA, while AS and HMMN take the light-meson DA results from Ref. [44].

Turning to the non-local charm-quark loop contributions, the fact that T_μ is inserted at the same place in the amplitude as A_μ is problematic: how can we disentangle a possible charm-quark loop contribution from a NP contribution to \mathcal{C}_7 or $\mathcal{C}_9^{\text{eff}}$? Over the years, this was the subject of intense (often acrimonious) debate. These non-local charm-quark contributions are particularly important in the region of charmonium resonances between the low- and large- q^2 regions, and may in principle affect observables such as branching ratios, S_i , R_{K^*} in the presence of NP, or P'_5 . A number of different approaches were used to tackle this problem. (i) The exchange of one soft gluon was computed within LCSR [42]. It was found that this contribution *increased* the size of the anomaly in P'_5 . (ii) Later on, a detailed next-to-leading-order computation was done in Ref. [45], but it was found that the correction to this leading-order result is very small. (iii) It is difficult to reliably compute the phase difference between the long-distance charm contribution and the short-distance physics. With this in mind, Ref. [41] conservatively introduced three nuisance parameters (one for each amplitude), to allow for constructive and destructive interference between the short-distance and long-distance charm contributions computed in Ref. [42]. This effectively increases the impact of the charm-quark loop contribution, reducing the anomaly. (iv) Another approach was to perform a fit to the resonances (in modulo and phase) and see if the tail of some resonance could explain the deviation in the anomaly bins [46]. (v) Finally, Ref. [47] adopted an approach based on a dispersive representation using the data on J/ψ and $\psi(2S)$ to determine the analytic structure of the correlation function of interest and its q^2 dependence (up to a polynomial). In all cases, it was found that it is not possible to explain the P'_5 anomaly with T_μ in the SM.

In Ref. [41], improved QCD factorization (QCDF) is used to include all of the above corrections. The amplitude is decomposed as [48]

$$\langle \ell^+ \ell^- \bar{K}_i^* | H_{\text{eff}} | \bar{B} \rangle = \sum_{a,\pm} C_{i,a} \xi_a + \Phi_{B,\pm} \otimes T_{i,a,\pm} \otimes \Phi_{K^*,a} + \mathcal{O}(\Lambda_{\text{QCD}}/m_B). \quad (9)$$

Here, $C_{i,a}$ and $T_{i,a}$ ($a = \perp, \parallel$) are perturbatively-computable contributions to the various K^* polarizations ($i = 0, \perp, \parallel$) and Φ_{B,K^*} stands for the light-cone DA of the B and K^* mesons. There are two types of corrections. First, there are the factorizable corrections that can be absorbed into the FFs. These include $\mathcal{O}(\alpha_s)$ and $\mathcal{O}(\Lambda_{\text{QCD}}/m_B)$ corrections. Second, there are nonfactorizable corrections that cannot be absorbed into the FFs. These also come in two types. There are those that originate from hard gluon exchange; these are calculable within QCDF (including insertions of the operators \mathcal{O}_{1-6} and \mathcal{O}_8 [48]). And there are those that are power corrections of $\mathcal{O}(\Lambda_{\text{QCD}}/m_B)$, which include the $c\bar{c}$

loops mentioned above. In Ref. [41], they are included using the computation of [42], but allowing for a constructive/destructive interference with the short-distance effect.

Finally, it is often stated that “LFUV observables are always clean.” However, this is only true in the SM because of certain cancellations. In the presence of NP, these cancellations do not occur. This is particularly visible in the case of R_{K^*} (see Fig. 3 in Ref. [49]). Thus, when considering NP, it is important to take into account the hadronic uncertainties (form factors and charm loops).

To recap, there are two sources of theoretical error in the EFT analysis of the B anomalies: form factors and the non-local charm-loop contributions. There has been great progress in the computations of FFs, using different approaches. In addition, the charm-loop contributions have been studied in full detail using different explicit computational methods. The theoretical error in the $b \rightarrow sl^+\ell^-$ anomaly is now under better control.

3.3 Global fits: results

When a global fit is performed, a hypothesis is made regarding which NP Wilson coefficients are allowed to vary. This fixes the number of parameters of a fit, n , and the number of degrees of freedom $N_{dof} = N_{obs} - n$, where N_{obs} is the number of observables. When the results are obtained, there are two statistical quantities of interest:

- (i) The p-value of a given hypothesis is a function of χ_{min}^2 and N_{dof} . This quantity is a measure of the goodness of the fit, i.e., it indicates whether or not the hypothesis provides a good fit. For example, the p-value of the SM fit to the $b \rightarrow sl^+\ell^-$ data is 1.1%, which corresponds to a disagreement at the level of $\sim 2.5\sigma$. If the p-value were to fall below 5σ , the SM would be excluded.
- (ii) Pull_{SM} provides very precise information on the comparison of the SM and a given NP hypothesis as explanations of the data: it tells us by how many σ s the SM hypothesis is disfavoured with respect to a given NP hypothesis. It is related to the difference of the χ_{min}^2 s of the two fits and to the difference in the N_{dof} . This allows us to quantitatively compare the Pull_{SM} s of hypotheses with different numbers of free parameters.

3.3.1 1D, 2D and 6D scenarios

We begin with global fits in which one NP WC is allowed to vary. These 1D fits provide useful information: they indicate if there is a WC (or constrained combination of WCs) in a given basis that is dominant in the explanations of the B anomalies. The three groups have all performed 1D fits, and there are two solutions that are most preferred by all of them: $\mathcal{C}_{9\mu}^{\text{NP}}$ and $\mathcal{C}_{9\mu}^{\text{NP}} = -\mathcal{C}_{10\mu}^{\text{NP}}$ ⁸. The results for the ΛCDMN , AS and HMMN groups are shown in Tables 1, 2 and 3, respectively.

⁸A third possible solution, $\mathcal{C}_{10\mu}^{\text{NP}}$, gives a very good description of the data in the LFUV fit. However, it fails to provide a good description of the data in the complete fit, particularly when compared with other NP hypotheses.

Above, we have pointed out the differences among the three groups as regards the methodology (particularly the number of observables included in the fit) and the choice of form factors. Despite these, the results in Tables 1, 2 and 3 are remarkably similar. Two types of fits were done: the complete fit, which includes all observables used by the individual groups, and the LFUV fit, which includes mainly observables sensitive to the breaking of lepton flavour universality. For the LFUV fit, the results are virtually identical. For the complete fit, the results of the ACDMN and HMMN groups are remarkably close. (The excellent agreement between these two different analyses also extends to higher-dimensional fits.) Tiny differences are due to the small difference in the number of observables (and the inclusion of the baryonic Λ_b decay in the HMMN analysis) and the different form factors. Still, the general agreement between these two analyses shows that these effects are rather marginal. On the other hand, there are greater differences with the AS result. AS find that the Pulls for the $\mathcal{C}_{9\mu}^{\text{NP}}$ and $\mathcal{C}_{9\mu}^{\text{NP}} = -\mathcal{C}_{10\mu}^{\text{NP}}$ hypotheses are smaller than for ACDMN and HMMN. Also, they find $\mathcal{C}_{9\mu}^{\text{NP}} = -\mathcal{C}_{10\mu}^{\text{NP}}$ has a marginally larger pull than $\mathcal{C}_{9\mu}^{\text{NP}}$, which is opposite to ACDMN and HMMN. This is almost certainly due to the smaller number of observables in the AS analysis – particularly the exclusion of the [6,8] bin in all observables⁹ – and, to a lesser extent, the inclusion of $\Lambda_b \rightarrow \Lambda\mu^+\mu^-$ at low-recoil¹⁰.

Although the two most-preferred NP explanations are $\mathcal{C}_{9\mu}^{\text{NP}}$ and $\mathcal{C}_{9\mu}^{\text{NP}} = -\mathcal{C}_{10\mu}^{\text{NP}}$, there are other 1D hypotheses that have significant Pulls. ACDMN find that $\mathcal{C}_{9\mu}^{\text{NP}} = -\mathcal{C}'_{9\mu}{}^{\text{NP}}$ has a large pull in the complete fit, which is about the same size as that of $\mathcal{C}_{9\mu}^{\text{NP}}$ and $\mathcal{C}_{9\mu}^{\text{NP}} = -\mathcal{C}_{10\mu}^{\text{NP}}$. However, this solution predicts $R_K \simeq 1$, as in the SM, so in the LFUV fit, its pull is 3.0σ , smaller than that of $\mathcal{C}_{9\mu}^{\text{NP}}$ and $\mathcal{C}_{9\mu}^{\text{NP}} = -\mathcal{C}_{10\mu}^{\text{NP}}$. For this reason, this solution is not favoured.

It is interesting to see how the Pulls of the 1D explanations to the $b \rightarrow s\ell^+\ell^-$ anomalies have evolved in the past eight years, as more observables, more experiments and better experimental and theoretical precision are included in each iteration. (Here we refer to Refs. [37, 38, 49, 53].) For the complete fit, the Pull_{SM} of $\mathcal{C}_{9\mu}^{\text{NP}}$ has been 4.5 [2016], 5.8 [2018], 5.6 [2019], 6.3 [2020], 7.0 [2021]. And for $\mathcal{C}_{9\mu}^{\text{NP}} = -\mathcal{C}_{10\mu}^{\text{NP}}$: 4.2 [2016], 5.3 [2018], 5.2 [2019], 5.8 [2020], 6.2 [2021]. In both cases, the size of the discrepancy with the SM of the $b \rightarrow s\ell^+\ell^-$ anomaly has steadily increased. Note that the hierarchy in Pulls between these two solutions is reversed if only the subset of LFUV observables is considered. A solution [54] to this apparent contradiction is discussed in the next subsection.

2D fits allow us to explore if, by permitting an extra NP Wilson coefficient (or a constrained combination) to vary, we get a better description of the data than with a single coefficient, or the improvement is negligible¹¹. For the 2D fits, we focus on the

⁹In contrast to $\mathcal{C}_{9\mu}$, the solution $\mathcal{C}_{9\mu} = -\mathcal{C}_{10\mu}$ produces a SM-like value for P'_5 in both anomaly bins [4,6] and [6,8] (see Fig. 5 in Ref. [38]). Since the [6,8] bin is problematic for the $\mathcal{C}_{9\mu} = -\mathcal{C}_{10\mu}$ solution, and since AS have excluded this bin from their fit, this might explain the preference of the AS fit for $\mathcal{C}_{9\mu} = -\mathcal{C}_{10\mu}$. Note that important progress has been made recently in explicit computations for the whole low- q^2 region.

¹⁰This mode shows an unexpected preference at low-recoil for $\mathcal{C}_{9\mu}^{\text{NP}} > 0$, in contradiction with the rest of the data. However, a recent reinterpretation excluding LEP data finds a result in nice agreement with the rest of the data: it shows a small deficit in this channel instead of an excess [33].

¹¹We stress that, because Pull_{SM} includes information about the N_{dof} , one can compare fits with different

ACDMN 1D Hyp.	Complete fit: 246 observables			LFUV + radiative + $B_s \rightarrow \mu^+ \mu^-$		
	Best fit	Pull _{SM} (σ)	p-value	Best fit	Pull _{SM} (σ)	p-value
$\mathcal{C}_{9\mu}^{\text{NP}}$	$-1.06^{+0.15}_{-0.14}$	7.0	39.5 %	$-0.82^{+0.22}_{-0.24}$	4.0	36.0 %
$\mathcal{C}_{9\mu}^{\text{NP}} = -\mathcal{C}_{10\mu}^{\text{NP}}$	$-0.44^{+0.07}_{-0.08}$	6.2	22.8 %	$-0.37^{+0.08}_{-0.09}$	4.6	68.0 %

Table 1: Analysis of the ACDMN group as of Moriond 2021: most preferred 1D patterns of NP in $b \rightarrow s\mu^+\mu^-$. For a complete set of 1D patterns, see Ref. [49]. The p -value of the SM hypothesis is 1.1% (corresponding to a discrepancy with the data of 2.5σ) for the complete fit and 1.4% for the LFUV fit.

AS 1D Hyp.	Complete fit: 130 observables		LFUV + $B_s \rightarrow \mu^+ \mu^-$	
	Best fit	Pull _{SM} (σ)	Best fit	Pull _{SM} (σ)
$\mathcal{C}_{9\mu}^{\text{NP}}$	-0.80 ± 0.14	5.7	$-0.74^{+0.20}_{-0.21}$	4.1
$\mathcal{C}_{9\mu}^{\text{NP}} = -\mathcal{C}_{10\mu}^{\text{NP}}$	-0.41 ± 0.07	5.9	-0.35 ± 0.08	4.6

Table 2: Analysis of the AS group as of Moriond 2021: most preferred 1D patterns of NP in $b \rightarrow s\mu^+\mu^-$, see Ref. [50], v2 [Apr.2021]. The number of observables is taken from Ref. [51]. Note: a revised Ref. [50], v3 [Sept.2021] finds very similar results: $\mathcal{C}_{9\mu}^{\text{NP}} = -0.73 \pm 0.15$ (Pull_{SM} = 5.2σ) and $\mathcal{C}_{9\mu}^{\text{NP}} = -\mathcal{C}_{10\mu}^{\text{NP}} = -0.39 \pm 0.07$ (5.6σ) for the complete fit, and unchanged results for the LFUV fit.

HMMN 1D Hyp.	Complete fit: 173 observables		only $R_{K^{(*)}} + B_{d,s} \rightarrow \mu^+ \mu^-$	
	Best fit	Pull _{SM} (σ)	Best fit	Pull _{SM} (σ)
$\mathcal{C}_{9\mu}^{\text{NP}}$	-0.95 ± 0.12	7.6	-0.77 ± 0.21	4.0
$\mathcal{C}_{9\mu}^{\text{NP}} = -\mathcal{C}_{10\mu}^{\text{NP}}$	-0.49 ± 0.08	6.7	-0.38 ± 0.09	4.6

Table 3: Analysis of the HMMN group as of Moriond 2021: most preferred 1D patterns of NP in $b \rightarrow s\mu^+\mu^-$. For a complete set of 1D patterns, see Ref. [52].

ACDMN analysis, but we note that AS and HMMN also perform 2D fits.

A number of 2D hypothesis are examined in Ref. [49]. Here we discuss two of them:

- a) Adding $\mathcal{C}_{10\mu}^{\text{NP}}$ to $\mathcal{C}_{9\mu}^{\text{NP}}$ slightly decreases the Pull_{SM} in the complete fit (Table 4). That is, the addition of this NP WC does not provide a better description of the data. Still, it is clear that a small contribution to $\mathcal{C}_{10\mu}^{\text{NP}}$ (or to $\mathcal{C}'_{10\mu}^{\text{NP}}$ or a scalar operator) is required to explain the small ($\sim 2\sigma$) deficit with respect to the SM observed in $\mathcal{B}(B_s \rightarrow \mu^+\mu^-)$. On the other hand, the recent experimental update by LHCb is closer to the SM value, and this has slightly reduced its significance: in the 2D [$\mathcal{C}_{9\mu}^{\text{NP}}, \mathcal{C}_{10\mu}^{\text{NP}}$] plot, $\mathcal{C}_{10\mu}^{\text{NP}}$ is now consistent with zero at 1σ .
- b) If instead a RH current with the structure $\mathcal{C}'_{9\mu} = -\mathcal{C}'_{10\mu}$ is added to $\mathcal{C}_{9\mu}$ (hypothesis 5 in notation of [38]), a better description of the data is found: this is the scenario with the largest Pull_{SM} (7.4σ), see Table 4. The same result is obtained if only $\mathcal{C}'_{10\mu}$ is added. The reason is that the RH current counterbalances the effect of a

N_{dof} .

too-large $\mathcal{C}_{9\mu}^{\text{NP}}$ contribution in R_K . On the other hand, if this RH current structure is added to the hypothesis $\mathcal{C}_{9\mu}^{\text{NP}} = -\mathcal{C}_{10\mu}^{\text{NP}}$ instead of $\mathcal{C}_{9\mu}^{\text{NP}}$, the description of the data is significantly worse with a reduction of nearly 1.5σ in Pull_{SM} (see hypothesis 4 in Ref. [49]).

ACDMN 2D Hyp.	Complete fit: 246 observables			LFUV + radiative		
	Best fit	$\text{Pull}_{\text{SM}} (\sigma)$	p-value	Best fit	$\text{Pull}_{\text{SM}} (\sigma)$	p-value
$(\mathcal{C}_{9\mu}^{\text{NP}}, \mathcal{C}_{10\mu}^{\text{NP}})$	(-1.00, +0.11)	6.8	39.4 %	(-0.12, +0.54)	4.3	65.6 %
$(\mathcal{C}_{9\mu}^{\text{NP}}, \mathcal{C}'_{10\mu}^{\text{NP}})$	(-1.26, -0.35)	7.4	55.9 %	(-1.82, -0.59)	4.7	84.1 %
Hyp. 4	(-0.48, +0.11)	6.0	24.0 %	(-0.46, +0.15)	4.5	74.5 %
Hyp. 5	(-1.26, +0.25)	7.4	55.8 %	(-2.08, +0.51)	4.7	86.0 %

Table 4: Analysis of the ACDMN group: most preferred 2D patterns of NP in $b \rightarrow s\mu^+\mu^-$. Hyp. 4 is $(\mathcal{C}_{9\mu}^{\text{NP}} = -\mathcal{C}_{10\mu}^{\text{NP}}, \mathcal{C}'_{9\mu}^{\text{NP}} = -\mathcal{C}'_{10\mu}^{\text{NP}})$, hyp. 5 is $(\mathcal{C}_{9\mu}^{\text{NP}}, \mathcal{C}'_{9\mu}^{\text{NP}} = -\mathcal{C}'_{10\mu}^{\text{NP}})$. For a complete set of 2D patterns, see Ref. [49].

ACDMN also performs a 6D fit¹², see Table 5. This shows consistency with the 1D and 2D fits, and confirms that $\mathcal{C}_{9\mu}^{\text{NP}}$ is the dominant NP WC. It is nonzero at more than 3σ , while all other WCs are consistent with zero at 1σ . Finally, we note that the Pull_{SM} for this 6D fit has increased in time: 5.1σ [2019], 5.8σ [2020] to 6.6σ in the most recent analysis of 2021.

ACDMN	$\mathcal{C}_7^{\text{NP}}$	$\mathcal{C}_{9\mu}^{\text{NP}}$	$\mathcal{C}_{10\mu}^{\text{NP}}$	$\mathcal{C}'_7^{\text{NP}}$	$\mathcal{C}'_{9\mu}^{\text{NP}}$	$\mathcal{C}'_{10\mu}^{\text{NP}}$
Best fit	+0.01	-1.21	+0.15	+0.01	+0.37	-0.21
1σ region	[-0.02, +0.04]	[-1.38, -1.01]	[+0.00, +0.34]	[-0.02, +0.03]	[-0.12, +0.80]	[-0.42, +0.02]

Table 5: Analysis of the ACDMN group: best-fit points and 1σ regions for the 6D hypothesis of NP in $b \rightarrow s\mu^+\mu^-$. The Pull_{SM} of this hypothesis is 6.6σ [49].

3.3.2 LFUV and LFU New Physics

As shown in Sec. 3.1, the $b \rightarrow s\ell^+\ell^-$ anomalies appear in two types of observables, those that involve only $b \rightarrow s\mu^+\mu^-$, and those that are LFUV. The scenarios of Sec. 3.3.1 assume that the NP affects only $b \rightarrow s\mu^+\mu^-$. In Ref. [54] (essentially the ACDMN group) a new NP scenario was explored. Just as there are two categories of observables, it was assumed that there are two types of NP, one LFUV, affecting only $b \rightarrow s\mu^+\mu^-$, the other lepton flavour universal (LFU), equally affecting all $b \rightarrow s\ell^+\ell^-$ processes, $\ell = e, \mu$ and τ . The LFUV NP then explains the LFUV observables, while the combination of LFUV and LFU NP explains the $b \rightarrow s\mu^+\mu^-$ observables.

The WCs of the LFUV and LFU NP are denoted $\mathcal{C}_{i\mu}^V$ and \mathcal{C}_i^U , respectively. The

¹²We note that HMMN does 10D and 20D fits [52].

transformation from the standard $(\mathcal{C}_{i\mu}, \mathcal{C}_{ie})$ basis to the new $(\mathcal{C}_{i\mu}^V, \mathcal{C}_i^U)$ basis is given by

$$\begin{aligned}\mathcal{C}_{i\mu} &= \mathcal{C}_{i\mu}^V + \mathcal{C}_i^U, \\ \mathcal{C}_{ie} &= \mathcal{C}_i^U,\end{aligned}\tag{10}$$

and similarly for τ . In Sec. 3.3.1, we saw that the complete fits prefer the NP scenario $\mathcal{C}_{9\mu}^{\text{NP}}$, while the LFUV fits prefer $\mathcal{C}_{9\mu}^{\text{NP}} = -\mathcal{C}_{10\mu}^{\text{NP}}$. This observation suggests looking at the 2D scenario¹³.

$$[\mathcal{C}_9^V = -\mathcal{C}_{10}^V, \mathcal{C}_9^U]\tag{11}$$

The global fit was performed with this hypothesis [49], and it was found that it is one of the most promising scenarios, with a Pull_{SM} of 7.3σ (scenario 8 in the notation of Ref. [54]). As expected, the first component nicely explains the LFUV observables, while the second universal contribution adds a necessary extra contribution to the $b \rightarrow s\mu^+\mu^-$ observables (but also $b \rightarrow se^+e^-$). This universal NP contribution helps in explaining all the anomalies (in optimized observables for $B \rightarrow K^*\mu^+\mu^-$ and $B_s \rightarrow \phi\mu^+\mu^-$) that the naive scenario $\mathcal{C}_{9\mu}^V = -\mathcal{C}_{10\mu}^V$ cannot explain alone. More examples of LFUV-LFU scenarios can be found in Refs. [38, 49, 54].

This idea is not dissimilar from the idea of allowing LFUV NP in $b \rightarrow s\mu^+\mu^-$ and $b \rightarrow se^+e^-$. Complete analyses of this type of explanation, including many different scenarios, can be found in Refs. [52, 55, 56].

In summary, for the ACDMN group, the title of “most promising NP scenario” is no longer a contest between the 1D hypotheses $\mathcal{C}_{9\mu}^{\text{NP}}$ and $\mathcal{C}_{9\mu}^{\text{NP}} = -\mathcal{C}_{10\mu}^{\text{NP}}$, but rather between two 2D hypotheses:

$$[\mathcal{C}_{9\mu}^{\text{NP}}, \mathcal{C}_{9\mu}^{\prime\text{NP}} = -\mathcal{C}_{10\mu}^{\text{NP}}] \quad \text{or} \quad [\mathcal{C}_9^V = -\mathcal{C}_{10}^V, \mathcal{C}_9^U]\tag{12}$$

Indeed, this confirms what was observed in the 1D fits: a vectorial coupling to leptons in the form of $\mathcal{C}_{9\mu}^{\text{NP}}$ (only for muons) or \mathcal{C}_9^V (universal) is required to have a good description of the data. In this sense, both hypotheses in Eq. (12) provide an excellent explanation for the two largest anomalies, R_K and P_5' , in contrast to $\mathcal{C}_{9\mu}^{\text{NP}} = -\mathcal{C}_{10\mu}^{\text{NP}}$, which was unable to explain P_5' (see Fig. 4 in Ref. [49]).

3.4 Scale of New Physics

Flavour observables are sensitive to higher scales than direct searches at colliders. Therefore, if NP affects flavour, it is not surprising that it would be seen first in this sector. This naturally leads to the question: What is the scale of NP required to explain the $b \rightarrow s\ell^+\ell^-$ anomalies? The answer to this question depends on the assumption we make about the size of the NP couplings and the way NP enters the $b \rightarrow s\ell^+\ell^-$ amplitude.

¹³For notational convenience, the subscript μ of the LFUV contribution is understood, and is not written explicitly.

As discussed in Sec. 2, the interaction of NP with the SM particles is described by the SMEFT. The dimension-6 four-fermion operators generated when the NP is integrated out are contained in the effective Hamiltonian $H_{eff}^{\text{NP}} = \sum \frac{\mathcal{O}_i}{\Lambda_i^2}$. Comparing this with Eq. (3) for three different cases, we find the following NP scales:

- $b \rightarrow s\ell^+\ell^-$ transitions induced at tree level, assuming $\mathcal{O}(1)$ couplings:

$$\Lambda_i^{\text{Tree}} = \frac{4\pi v}{s_w g} \frac{1}{\sqrt{2|V_{tb}V_{ts}^*|}} \frac{1}{|C_i^{\text{NP}}|^{1/2}} \sim \frac{35 \text{ TeV}}{|C_i^{\text{NP}}|^{1/2}}, \quad (13)$$

- $b \rightarrow s\ell^+\ell^-$ transitions induced at loop level, assuming $\mathcal{O}(1)$ couplings:

$$\Lambda_i^{\text{Loop}} \sim \frac{35 \text{ TeV}}{4\pi|C_i^{\text{NP}}|^{1/2}} \sim \frac{3 \text{ TeV}}{|C_i^{\text{NP}}|^{1/2}}, \quad (14)$$

- Minimal Flavour Violation with CKM-SM: There is a further reduction of 1/5 in the NP scale due to $\sqrt{|V_{tb}V_{ts}^*|} \sim 1/5$.

In all cases, if the NP coupling is less than $\mathcal{O}(1)$, the NP scale Λ is reduced correspondingly.

Turning to the $b \rightarrow c\tau\nu$ anomalies, this transition takes place at tree level in the SM. As we will see below, an explanation requires a rather large $\mathcal{O}(10\%)$ tree-level NP contribution at the amplitude level. This implies that

$$\Lambda^{\text{NP}} \sim 1/(\sqrt{2}G_F|V_{cb}|0.10)^{1/2} \sim 4 \text{ TeV}. \quad (15)$$

3.5 Mapping WET to SMEFT

In the fits we have determined which operators must receive NP contributions in order to reproduce the data. There are two types of solutions: (i) pure LFUV, with NP only in $b \rightarrow s\mu^+\mu^-$, and (ii) $b \rightarrow s\mu^+\mu^-$ LFUV + LFU contributions. In both cases, the question now is: what kinds of NP can generate these solutions? In this subsection, we examine general features of such NP – this is the “model-independent” model analysis. Specific models will be examined in the next subsection.

As discussed in Sec. 2, the EFT used in the fits is the WET. It is appropriate for physics at the scale m_b : it is invariant under $SU(3)_C \times U(1)_{em}$ and all particles with masses greater than m_b have been integrated out. On the other hand, the EFT generated at high energies when the heavy NP particles have been integrated out is the SMEFT. A first step in identifying what kinds of NP can be responsible for the $b \rightarrow s\ell^+\ell^-$ anomalies comes by mapping WET onto SMEFT, focusing on $\mathcal{O}_{9,10}^{(\ell)}$.

In the SMEFT, the dimension-6 operators that contribute to these WCs at tree level can be separated into two categories: LFUV and LFU. The LFUV operators are a subset

of the semileptonic four-fermion operators. A simple basis for these operators is [57]

$$\begin{aligned}
\mathcal{O}_{LQ}^{(1)} &= (\bar{L}_i \gamma_\mu L_j)(\bar{Q}_k \gamma^\mu Q_l) , \\
\mathcal{O}_{LQ}^{(3)} &= (\bar{L}_i \gamma_\mu \sigma^I L_j)(\bar{Q}_k \gamma^\mu \sigma^I Q_l) , \\
\mathcal{O}_{Qe} &= (\bar{Q}_i \gamma_\mu Q_j)(\bar{e}_k \gamma^\mu e_l) , \\
\mathcal{O}_{Ld}^{(1)} &= (\bar{L}_i \gamma_\mu L_j)(\bar{d}_k \gamma^\mu d_l) , \\
\mathcal{O}_{ed}^{(1)} &= (\bar{e}_i \gamma_\mu e_j)(\bar{d}_k \gamma^\mu d_l) ,
\end{aligned} \tag{16}$$

where i, j, k, l are flavour (generation) indices. These are LFV for $i \neq j$, but for those that are LFC, one sees that they can be LFUV since the $ij = ee, \mu\mu$ and $\tau\tau$ WCs are not necessarily equal. It is convenient to combine the first two operators: $\mathcal{O}_{LQ}^{(1,3)} \equiv \mathcal{O}_{LQ}^{(1)} + \mathcal{O}_{LQ}^{(3)}$. These four SMEFT operators contribute to the four $b \rightarrow s\mu^+\mu^-$ WCs as follows [58]:

$$\begin{aligned}
\mathcal{C}_{9\mu}^{\text{NP}} &= \frac{\pi v^2}{\alpha \Lambda^2} \left[\tilde{\mathcal{C}}_{LQ}^{(1,3)\mu\mu 23} + \tilde{\mathcal{C}}_{Qe}^{23\mu\mu} \right] , \\
\mathcal{C}_{10\mu}^{\text{NP}} &= \frac{\pi v^2}{\alpha \Lambda^2} \left[\tilde{\mathcal{C}}_{Qe}^{23\mu\mu} - \tilde{\mathcal{C}}_{LQ}^{(1,3)\mu\mu 23} \right] , \\
\mathcal{C}'_{9\mu}{}^{\text{NP}} &= \frac{\pi v^2}{\alpha \Lambda^2} \left[\tilde{\mathcal{C}}_{Ld}^{\mu\mu 23} + \tilde{\mathcal{C}}_{ed}^{\mu\mu 23} \right] , \\
\mathcal{C}'_{10\mu}{}^{\text{NP}} &= \frac{\pi v^2}{\alpha \Lambda^2} \left[\tilde{\mathcal{C}}_{ed}^{\mu\mu 23} - \tilde{\mathcal{C}}_{Ld}^{\mu\mu 23} \right] ,
\end{aligned} \tag{17}$$

where $\tilde{\mathcal{C}}$ indicates a SMEFT WC at low energies, below the scale of electroweak symmetry breaking. The $\tilde{\mathcal{C}}$ s are related to high-energy SMEFT WCs using renormalization-group running. We stress that the above relations hold only for the basis of Eq. (16).

Recall that the preferred 1D fits involve $\mathcal{C}_{9\mu}^{\text{NP}}$ or $\mathcal{C}_{9\mu}^{\text{NP}} = -\mathcal{C}_{10\mu}^{\text{NP}}$ (Tables 1, 2 and 3). Consider the second solution. This arises if $\tilde{\mathcal{C}}_{Qe}^{23\mu\mu} = 0$. In this case, $\mathcal{C}_{9\mu}^{\text{NP}} + \mathcal{C}_{10\mu}^{\text{NP}} = 0$; the only nonzero WC is

$$\mathcal{C}_{9\mu}^{\text{NP}} - \mathcal{C}_{10\mu}^{\text{NP}} = 2 \frac{\pi v^2}{\alpha \Lambda^2} \tilde{\mathcal{C}}_{LQ}^{(1,3)\mu\mu 23} . \tag{18}$$

This solution is particularly good for model building. There is only one WC and its presence does not require any special relations between independent SMEFT operators. Also, it has a simple physical interpretation: the NP couples only to LH fermions.

Compare this with the first solution, $\mathcal{C}_{9\mu}^{\text{NP}}$. In order for it to be the only nonzero WC, it is necessary that $\mathcal{C}_{10\mu}^{\text{NP}} = 0$, which requires that

$$\tilde{\mathcal{C}}_{LQ}^{(1,3)\mu\mu 23} = \tilde{\mathcal{C}}_{Qe}^{23\mu\mu} . \tag{19}$$

Since the operators are independent, their coefficients are generally unrelated; any such relation requires additional explanation, such as a symmetry.

In the particular case of $\mathcal{C}_{9\mu}^{\text{NP}}$, such a symmetry is not difficult to find. While the operators $\mathcal{O}_{LQ}^{(1,3)}$ and \mathcal{O}_{Qe} both involve LH quarks, they involve LH and RH charged leptons,

respectively. For NP in $b \rightarrow s\mu^+\mu^-$ decays, if its couplings are invariant under L_μ (the μ lepton number), it will couple equally to μ_L and μ , and its effects will be seen in $\mathcal{C}_{9\mu}^{\text{NP}}$.

The point here is that it is possible to find single-particle NP models for each of the 1D solutions of the EFT analysis, $\mathcal{C}_{9\mu}^{\text{NP}}$ and $\mathcal{C}_{9\mu}^{\text{NP}} = -\mathcal{C}_{10\mu}^{\text{NP}}$. Considerations of SMEFT help to accomplish this.

For the 2D fits, the preferred scenarios are $(\mathcal{C}_{9\mu}^{\text{NP}}, \mathcal{C}_{10\mu}^{\text{NP}})$ and $(\mathcal{C}_{9\mu}^{\text{NP}}, \mathcal{C}'_{9\mu}{}^{\text{NP}} = -\mathcal{C}_{10\mu}^{\text{NP}})$ (see Table 4). There is no problem with the second scenario. As discussed above, $\mathcal{C}_{9\mu}^{\text{NP}}$ can be produced by NP that obeys a symmetry under which μ_L and μ_R transform in the same way, and $\mathcal{C}'_{9\mu}{}^{\text{NP}} = -\mathcal{C}_{10\mu}^{\text{NP}}$ is already an SMEFT WC. On the other hand, the first solution is more complicated. First, in order to produce $\mathcal{C}'_{10\mu}{}^{\text{NP}}$, one requires NP that obeys a symmetry under which μ_L and μ_R transform in the *opposite* way. That is, two different NP particles are required: the exchange of one generates $\mathcal{C}_{9\mu}^{\text{NP}}$, and the other generates $\mathcal{C}'_{10\mu}{}^{\text{NP}}$. Second, it is not obvious what is the symmetry under which μ_L and μ_R transform equally but oppositely.

Finally, the scenario in the 6D fit (Table 5) is acceptable from a model-building point of view, and all WCs can be written in SMEFT form using the following combinations: $\mathcal{C}_{9\mu}^{\text{NP}} \pm \mathcal{C}_{10\mu}^{\text{NP}}$, $\mathcal{C}'_{9\mu}{}^{\text{NP}} \pm \mathcal{C}'_{10\mu}{}^{\text{NP}}$, $\mathcal{C}'_{7\mu}{}^{\text{NP}}$, $\mathcal{C}_{7\mu}^{\text{NP}}$.

Turning to LFU SMEFT operators that contribute to $b \rightarrow s\ell^+\ell^-$, there are three dimension-6 operators involving the Higgs field [57]:

$$\begin{aligned}\mathcal{O}_{\varphi Q}^{(1)} &= (\varphi^\dagger i \overleftrightarrow{D}_\mu \varphi)(\bar{Q}_i \gamma^\mu Q_j), \\ \mathcal{O}_{\varphi Q}^{(3)} &= (\varphi^\dagger i \overleftrightarrow{D}_\mu^I \varphi)(\bar{Q}_i \tau^I \gamma^\mu Q_j), \\ \mathcal{O}_{\varphi d} &= (\varphi^\dagger i \overleftrightarrow{D}_\mu \varphi)(\bar{d}_i \gamma^\mu d_j).\end{aligned}\tag{20}$$

These generate the following LFU NP contributions [58]:

$$\begin{aligned}\mathcal{C}_9^{\text{NP}} &= \frac{\pi v^2}{\alpha \Lambda^2} \left[\tilde{\mathcal{C}}_{\varphi Q}^{(1)23} + \tilde{\mathcal{C}}_{\varphi Q}^{(3)23} \right] (-1 + 4 \sin^2 \theta_W), \\ \mathcal{C}_{10}^{\text{NP}} &= \frac{\pi v^2}{\alpha \Lambda^2} \left[\tilde{\mathcal{C}}_{\varphi Q}^{(1)23} + \tilde{\mathcal{C}}_{\varphi Q}^{(3)23} \right], \\ \mathcal{C}'_9{}^{\text{NP}} &= \frac{\pi v^2}{\alpha \Lambda^2} \tilde{\mathcal{C}}_{\varphi d}^{23} (-1 + 4 \sin^2 \theta_W), \\ \mathcal{C}'_{10}{}^{\text{NP}} &= \frac{\pi v^2}{\alpha \Lambda^2} \tilde{\mathcal{C}}_{\varphi d}^{23}.\end{aligned}\tag{21}$$

The preferred LFUV + LFU solution involves $\mathcal{C}_{9\mu}^{\text{V}} = -\mathcal{C}_{10\mu}^{\text{V}}$ and \mathcal{C}_9^{U} . From the above, we see that $\mathcal{C}_9^{\text{NP}} \propto \mathcal{C}_{10}^{\text{NP}}$, so that it is not possible to produce only \mathcal{C}_9^{U} with the operators of Eq. (20).

However, there is another possibility. The full matching of WET to SMEFT must take into account loop effects and renormalization-group running. In particular, a low-energy \mathcal{C}_9^{U} can be generated via a loop-level process [59]. The fermion in the loop can be $u_{1,2}$, $d_{1,2,3}$ or τ [38, 59, 60, 61]. (For $u_3 = t$, a large ditop-dimuon coupling is disfavoured by EW precision tests [62].) For loops with u or d , it must be checked that these are compatible

with constraints from dijet searches and non-leptonic decays. On the other hand, the case where the fermion is a τ (see Fig. 1) is particularly interesting [38, 63] because it suggests a possible link between NP in the $b \rightarrow s\mu^+\mu^-$ and $b \rightarrow c\tau^-\bar{\nu}_\tau$ transitions. The key point here is that, if there is a $\mathcal{C}_{9\mu}^V = -\mathcal{C}_{10\mu}^V$ contribution to $b \rightarrow s\mu^+\mu^-$, it is not difficult to generate \mathcal{C}_9^U via a large $b \rightarrow s\tau\tau$ effective coupling. Through radiative effects by closing the loop of the operator $b \rightarrow s\tau^+\tau^-$, a NP contribution to \mathcal{C}_9^U is induced [38]:

$$\mathcal{C}_9^U \simeq 7.5 \left(1 - \sqrt{\frac{R_{D^{(*)}}}{R_{D^{(*)}SM}}} \right) \left(1 + \frac{\log(\Lambda^2/(1\text{TeV}^2))}{10.5} \right) \quad (22)$$

where Λ is the scale of NP that is taken in a range between 1 to 10 TeV.

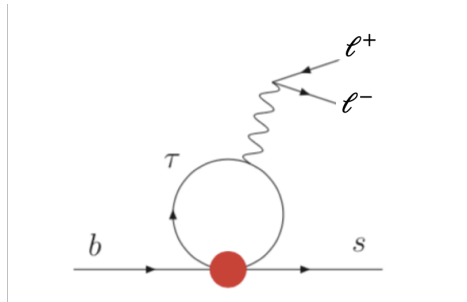


Figure 1: Diagram inducing a lepton universal contribution to \mathcal{C}_9^U through a τ loop.

3.6 Models

Many models have been proposed to explain the $b \rightarrow s\mu^+\mu^-$ anomalies. Some are “simplified models,” in which NP particles are added, but without giving any details of the underlying high-energy NP model from which these particles arise (the UV completion). Others do present full models, including the full gauge group and its particle content. In the simplest models (simplified or full), there is a single NP particle that contributes at tree level to $b \rightarrow s\mu^+\mu^-$. More complicated models typically involve many NP particles; some of them, but not all, contribute to $b \rightarrow s\mu^+\mu^-$.

In this review, we describe only the simplest models for all the anomalies. There are several reasons. First, there is the general prejudice that Nature prefers simple solutions (although this should not be taken as a golden rule). But there are also practical reasons. The complicated NP models have many new particles and generally have to satisfy many constraints. They are often viable only in a region of parameter space. But the data have changed over the years, so it is no longer clear whether these models are still valid. In contrast, the simplest models have been studied by several different groups and have been continually updated. (In fact, some of the early simple models have now been ruled out.) So we are certain that the models we describe here do actually explain the 2021 data.

For $b \rightarrow s\mu^+\mu^-$, there are two classes of simple models. They involve the tree-level exchange of a Z' or a leptoquark (LQ). These are described below.

3.6.1 Z' models

In Z' models, the Z' couples to both $\bar{s}b$ and $\mu^+\mu^-$. Given that it contributes to $\mathcal{C}_{9\mu}^{\text{NP}}$ or $\mathcal{C}_{9\mu}^{\text{NP}} = -\mathcal{C}_{10\mu}^{\text{NP}}$, the Z' coupling to $\bar{s}b$ is purely LH, but it may couple to both LH and RH $\mu^+\mu^-$ pairs.

We write the general couplings of the Z' as

$$\left[g_{ij}^Q (\bar{Q}_i \gamma^\mu Q_j) + g_{ij}^L (\bar{L}_i \gamma^\mu L_j) + g_{ij}^e (\bar{e}_i \gamma^\mu e_j) \right] Z'_\mu . \quad (23)$$

For $b \rightarrow s\mu^+\mu^-$, we are interested in those terms whose coefficients in the mass basis are g_{23}^Q , g_{22}^L and g_{22}^e . When the Z' is integrated out, one generates the following four-fermion operators relevant for $2q2\ell$ processes (two quarks and two leptons):

$$\mathcal{L}_{Z'}^{2q2\ell} = -\frac{g_{23}^Q g_{22}^L}{M_{Z'}^2} (\bar{s}_L \gamma^\mu b_L) (\bar{L}_\mu \gamma^\mu L_\mu) - \frac{g_{23}^Q g_{22}^e}{M_{Z'}^2} (\bar{s}_L \gamma^\mu b_L) (\bar{\mu}_R \gamma^\mu \mu) . \quad (24)$$

Both terms contribute to $b \rightarrow s\mu^+\mu^-$, while the first also contributes to $b \rightarrow s\bar{\nu}_\mu\nu_\mu$. If the $b \rightarrow s\mu^+\mu^-$ anomalies are explained by $\mathcal{C}_{9\mu}^{\text{NP}}$ alone, then $g_{22}^e = g_{22}^L$, while $g_{22}^e = 0$ if $\mathcal{C}_{9\mu}^{\text{NP}} = -\mathcal{C}_{10\mu}^{\text{NP}}$.

In addition to $2q2\ell$ operators, Z' exchange also produces four-quark ($4q$) and four-lepton (4ℓ) operators at tree level. The operators constructed from the same currents as above are

$$\begin{aligned} \mathcal{L}_{\text{NP}}^{4q} &= -\frac{(g_{23}^Q)^2}{2M_{Z'}^2} (\bar{s}_L \gamma^\mu b_L) (\bar{s}_L \gamma_\mu b_L) , \\ \mathcal{L}_{\text{NP}}^{4\ell} &= -\frac{(g_{22}^L)^2}{2M_{Z'}^2} (\bar{L}_\mu \gamma^\mu L_\mu) (\bar{L}_\mu \gamma_\mu L_\mu) - \frac{g_{22}^L g_{22}^e}{2M_{Z'}^2} (\bar{L}_\mu \gamma^\mu L_\mu) (\bar{\mu}_R \gamma_\mu \mu) . \end{aligned} \quad (25)$$

The operator in $\mathcal{L}_{\text{NP}}^{4q}$ contributes to $B_s^0-\bar{B}_s^0$ mixing, while those in $\mathcal{L}_{\text{NP}}^{4\ell}$ contribute to neutrino trident production ($\nu_\mu N \rightarrow \nu_\mu N \mu^+\mu^-$) [64].

The point here is that the best-fit values of $\mathcal{C}_{9\mu}^{\text{NP}}$ or $\mathcal{C}_{9\mu}^{\text{NP}} = -\mathcal{C}_{10\mu}^{\text{NP}}$ place a constraint on $g_{23}^Q g_{22}^L / M_{Z'}^2$. This same quantity is also constrained by $b \rightarrow s\bar{\nu}_\mu\nu_\mu$.¹⁴ In addition, there are constraints on $(g_{23}^Q)^2 / M_{Z'}^2$ from $B_s^0-\bar{B}_s^0$ mixing, and on $(g_{22}^L)^2 / M_{Z'}^2$ from neutrino trident production. It must be checked that all these constraints are consistent with one another (for example, see Ref. [67]). This type of analysis is necessary for models, but not for EFTs.

Finally, there is an extremely important constraint coming from direct searches for Z' bosons in the process $pp \rightarrow Z' \rightarrow \mu^+\mu^-$ [68]. The translation of the experimental limit into a model constraint is completely model-dependent. It depends on how the Z' couples to all the quarks, and what is the branching ratio of $Z' \rightarrow \mu^+\mu^-$. This latter quantity can be affected if the Z' can also decay into dark matter, for example.

¹⁴The decay $b \rightarrow s\bar{\nu}_\mu\nu_\mu$ is analyzed within the SM in Ref. [65]; experimental results are given in Ref. [66].

All Z' models must take into account all of these constraints. (Furthermore, if one is interested in a particular Z' model, it may be necessary to update the constraint analysis, to see if the model is still viable.)

Many Z' models have been proposed to explain the $b \rightarrow s\mu^+\mu^-$ anomalies. The following list includes most of them, separated into four categories: the Z' is heavy and contributes to (i) $\mathcal{C}_{9\mu}^{\text{NP}}$, (ii) $\mathcal{C}_{9\mu}^{\text{NP}} = -\mathcal{C}_{10\mu}^{\text{NP}}$, or (iii) $\mathcal{C}_{9\mu}^{\text{NP}}$ and $\mathcal{C}_{10\mu}^{\text{NP}}$; (iv) light Z' bosons.

1. $\mathcal{C}_{9\mu}^{\text{NP}}$. As argued earlier, this NP explanation can arise only if the relation in Eq. (19) holds, which generally requires an additional symmetry. L_μ (the μ lepton number) is such a symmetry, but by itself it is not anomaly-free; an additional symmetry is required. The most popular choice is a gauged $L_\mu - L_\tau$ symmetry: Z' models with a $U(1)_{L_\mu - L_\tau}$ symmetry can be found in Refs. [69, 70, 71, 72, 73, 74, 75, 76, 77, 78, 79, 80, 197]. There are many variants in which the $U(1)$ has a different symmetry, but always includes L_μ , see Refs. [82, 83, 84, 85, 86, 87, 88, 89, 90]. Other frameworks include the 3-3-1 model with $\beta = -\sqrt{3}$ [91, 92] and Branco-Grimus-Lavoura (BGL) models [93].
2. $\mathcal{C}_{9\mu}^{\text{NP}} = -\mathcal{C}_{10\mu}^{\text{NP}}$. A variety of models have been proposed in which it is simply assumed that the Z' couples only to LH fermions (like the W^\pm in the SM). These can be found in Refs. [94, 95, 96, 97, 98, 99, 100, 101, 102, 103, 104, 105].
3. $\mathcal{C}_{9\mu}^{\text{NP}}$ and $\mathcal{C}_{10\mu}^{\text{NP}}$. There are other models in which the Z' couplings involve both $\mathcal{C}_{9\mu}^{\text{NP}}$ and $\mathcal{C}_{10\mu}^{\text{NP}}$. The relative size of the two WCs is dictated by some underlying dynamics of the model, see Refs. [106, 107, 108, 109, 110, 111, 112].
4. Light Z' bosons. In the above models, $M_{Z'} = O(\text{TeV})$ is assumed. But this is not necessarily required. In Refs. [97, 113, 114, 115, 116], scenarios are presented in which the Z' has a mass of a few GeV. (The couplings are also reduced so as to reproduce the preferred values of $\mathcal{C}_{9,10\mu}^{\text{NP}}$.)

3.6.2 LQ models

There are five spin-0 and five spin-1 LQs, denoted Δ and V respectively, with couplings [117]

$$\begin{aligned}
\mathcal{L}_\Delta &= (y_{Lu}\bar{L}u + y_{eQ}\bar{e}i\tau_2Q)\Delta_{-7/6} + y_{Ld}\bar{L}d\Delta_{-1/6} + (y_{LQ}\bar{L}^c i\tau_2Q + y_{eu}\bar{e}^c u)\Delta_{1/3} \\
&\quad + y_{ed}\bar{e}^c d\Delta_{4/3} + y'_{LQ}\bar{L}^c i\tau_2\bar{\tau}Q \cdot \vec{\Delta}'_{1/3} + h.c. \\
\mathcal{L}_V &= (g_{LQ}\bar{L}\gamma_\mu Q + g_{ed}\bar{e}\gamma_\mu d)V_{-2/3}^\mu + g_{eu}\bar{e}\gamma_\mu uV_{-5/3}^\mu + g'_{LQ}\bar{L}\gamma_\mu\bar{\tau}Q \cdot \vec{V}_{-2/3}^\mu \\
&\quad + (g_{Ld}\bar{L}\gamma_\mu d^c + g_{eQ}\bar{e}\gamma_\mu Q^c)V_{-5/6}^\mu + g_{Lu}\bar{L}\gamma_\mu u^c V_{1/6}^\mu + h.c. \tag{26}
\end{aligned}$$

$V_{-5/3}^\mu$ and $V_{1/6}^\mu$ do not couple to down-type quarks, and so are not of interest to us. The other LQs transform as follows under $SU(3)_c \times SU(2)_L \times U(1)_Y$:

$$\begin{aligned}
R_2 &\equiv \Delta_{-7/6} : (\bar{3}, 2, -7/6) \quad , \quad \tilde{R}_2 \equiv \Delta_{-1/6} : (\bar{3}, 2, -1/6) \quad , \quad S_1 \equiv \Delta_{1/3} : (\bar{3}, 1, 1/3) \quad , \\
&\quad \tilde{S}_1 \equiv \Delta_{4/3} : (\bar{3}, 1, 4/3) \quad , \quad S_3 \equiv \tilde{\Delta}'_{1/3} : (\bar{3}, 3, 1/3) \quad , \quad (27) \\
U_1 &\equiv V_{-2/3}^\mu : (\bar{3}, 1, -2/3) \quad , \quad U_3 \equiv \vec{V}_{-2/3}^\mu : (\bar{3}, 3, -2/3) \quad , \quad V_2 \equiv V_{-5/6}^\mu : (\bar{3}, 2, -5/6) \quad .
\end{aligned}$$

Note that here the hypercharge is defined as $Y = Q_{em} - I_3$. R_2 , \tilde{R}_2 , etc. are the names given to these LQs in Ref. [118]. We adopt this nomenclature here.

All of these LQs were explored at different times as potential explanations of the $b \rightarrow s\mu^+\mu^-$ anomalies. In Ref. [67], fits were done including each LQ individually, and it was found that only S_3 , U_1 and U_3 provide good fits. (The S_3 , U_1 and U_3 LQs were originally examined in Refs. [119, 120, 121, 122], [123, 124] and [125], respectively.) In the case of the U_1 , the best fit has $g_{ed}^{\mu b} \simeq 0$, so that all three LQ solutions have $\mathcal{C}_{9\mu}^{\text{NP}} = -\mathcal{C}_{10\mu}^{\text{NP}}$.

We therefore see that the $\mathcal{C}_{9\mu}^{\text{NP}} = -\mathcal{C}_{10\mu}^{\text{NP}}$ explanation can be generated by a Z' or a LQ, while the $\mathcal{C}_{9\mu}^{\text{NP}}$ solution is purely Z' .¹⁵ Ref. [67], it was shown that measurements of CP violation in $B \rightarrow K^*\mu^+\mu^-$ have the potential to distinguish the $\mathcal{C}_{9\mu}^{\text{NP}}$ and $\mathcal{C}_{9\mu}^{\text{NP}} = -\mathcal{C}_{10\mu}^{\text{NP}}$ explanations. Similarly, it was argued in Ref. [126] that these two solutions can be differentiated through the measurements of $\mathcal{B}(B_s \rightarrow \mu^+\mu^-)$ and CP-averaged azimuthal-angle asymmetries in $B \rightarrow K^*\mu^+\mu^-$.

4 Charged-current anomalies: $b \rightarrow c\ell^-\bar{\nu}_\ell$

We now turn to the charged-current B flavour anomalies, observed in $b \rightarrow c\ell^-\bar{\nu}_\ell$ transitions. Whereas $b \rightarrow s\ell^+\ell^-$ occurs at loop level in the SM, $b \rightarrow c\ell^-\bar{\nu}_\ell$ is a tree-level decay in the SM (although the amplitude is multiplied by $V_{cb} \simeq 0.04$). Thus, a larger (tree-level) NP contribution is required to explain these anomalies. On the other hand, a similarity with the neutral-current anomalies is that both have been seen in LFUV observables.

4.1 Experimental Results

Discrepancies with the SM have been seen in the following observables:

$$R_{D^{(*)}} \equiv \frac{\mathcal{B}(\bar{B} \rightarrow D^{(*)}\tau^-\bar{\nu}_\tau)}{\mathcal{B}(\bar{B} \rightarrow D^{(*)}\ell^-\bar{\nu}_\ell)} \quad , \quad \ell = e, \mu \quad , \quad R_{J/\psi} \equiv \frac{\mathcal{B}(B_c \rightarrow J/\psi\tau\nu_\tau)}{\mathcal{B}(B_c \rightarrow J/\psi\mu\nu_\mu)} \quad . \quad (28)$$

The latest results are (the $R_{D^{(*)}}$ numbers are taken from Ref. [127], the $R_{J/\psi}$ numbers from Ref. [128])

$$\begin{aligned}
R_D^{\tau/\ell} / (R_D^{\tau/\ell})_{\text{SM}} &= 1.14 \pm 0.10 \quad , \quad R_{D^*}^{\tau/\ell} / (R_{D^*}^{\tau/\ell})_{\text{SM}} = 1.14 \pm 0.06 \quad , \\
R_{J/\psi}^{\tau/\mu} / (R_{J/\psi}^{\tau/\mu})_{\text{SM}} &= 2.51 \pm 0.97 \quad . \quad (29)
\end{aligned}$$

¹⁵ Producing the $\mathcal{C}_{9\mu}^{\text{NP}}$ solution with LQs requires multiple LQs, whose couplings and masses are exceedingly fine-tuned.

The combined R_D and R_{D^*} results differ from the SM by 3.1σ .

The above results suggest the presence of NP in $b \rightarrow c\ell^-\bar{\nu}_\ell$ decays, but it is not clear which of $\ell = e, \mu$ and/or τ is affected. However, it has also been found that

$$R_{D^*}^{e/\mu}/(R_{D^*}^{e/\mu})_{\text{SM}} = 1.04 \pm 0.05 . \quad (30)$$

With this result, the simplest assumption is that NP mainly affects $b \rightarrow c\tau^-\bar{\nu}_\tau$, and most analyses focus on this scenario. With this in mind, two other relevant observables $B \rightarrow D^*\tau\nu_\tau$ are the τ polarization asymmetry $P_\tau(D^*)$ and the longitudinal D^* polarization $F_L(D^*)$:

$$P_\tau(D^*) \equiv \frac{\Gamma(B \rightarrow D^*\tau^{\lambda=+1/2}\nu_\tau) - \Gamma(B \rightarrow D^*\tau^{\lambda=-1/2}\nu_\tau)}{\Gamma(B \rightarrow D^*\tau\nu_\tau)} ,$$

$$F_L(D^*) \equiv \frac{\Gamma(B \rightarrow D_L^*\tau\nu_\tau)}{\Gamma(B \rightarrow D^*\tau\nu_\tau)} . \quad (31)$$

$P_\tau(D^*)$ and $F_L(D^*)$ were measured in Refs. [129, 130] and [131], respectively:

$$P_\tau(D^*) = -0.38 \pm 0.51_{-0.16}^{+0.21} , \quad F_L(D^*) = 0.60 \pm 0.08 \pm 0.035 . \quad (32)$$

These observables are useful for distinguishing NP explanation with different Lorentz structures. The unexpectedly large value observed for $F_L(D^*)$ suggested to look for alternative ways to measure it (see [132]).

Finally, there is also the observable $\mathcal{B}(B_c \rightarrow \tau\nu_\tau)$, which has not yet been measured. In Ref. [133] [Nov., 2016], it is argued that $\mathcal{B}(B_c \rightarrow \tau\nu_\tau) < 30\%$ is required for compatibility with the B_c lifetime. This disfavors NP contributions to $b \rightarrow c\tau^-\bar{\nu}_\tau$ with scalar couplings. In Ref. [134] [Aug., 2017], it is claimed that LEP data requires $\mathcal{B}(B_c \rightarrow \tau^-\bar{\nu}_\tau) < 10\%$, placing an even stronger constraint on these NP scenarios. On the other hand, this question was re-examined in Ref. [135] [May, 2019], and it was concluded that the constraint $\mathcal{B}(B_c \rightarrow \tau^-\bar{\nu}_\tau) < 10\%$ is not justified. A conservative analysis yields $\mathcal{B}(B_c \rightarrow \tau^-\bar{\nu}_\tau) < 60\%$, removing the constraint on NP with scalar couplings. At the present time, the value of the allowed upper limit on $\mathcal{B}(B_c \rightarrow \tau^-\bar{\nu}_\tau)$ is an important open question. Of course, this could be resolved if this branching ratio were measured.

In the above, we have always assumed lepton flavour conservation (LFC), writing the leptons in the final state as $\tau^-\bar{\nu}_\tau, \mu^-\bar{\nu}_\mu$, etc. This is done principally because this is how the experimental results have been reported. However, it should be remembered that, if NP is present, LFC might not be followed. (On the other hand, in the SM, one *does* have LFC, so only NP couplings that obey LFC can interfere with the SM.)

4.2 EFT analysis

Because the $\bar{\nu}$ in $b \rightarrow c\ell^-\bar{\nu}_\ell$ decays is not detected, we know nothing about its properties. In particular, we don't know if it is LH or RH. The case of a RH final-state neutrino will be addressed in the model analysis below; EFT analyses assume LH neutrinos.

With this assumption, and assuming that it is $b \rightarrow c\tau^-\bar{\nu}_\tau$ decays that receive NP contributions, the most general effective Hamiltonian for this decay is¹⁶

$$H_{\text{eff}} = \frac{4G_F}{\sqrt{2}} V_{cb} [(1 + C_V^L)O_V^L + C_V^R O_V^R + C_S^R O_S^R + C_S^L O_S^L + C_T O_T] , \quad (33)$$

with

$$\begin{aligned} O_V^L &= (\bar{c}\gamma^\mu P_L b)(\bar{\tau}\gamma_\mu P_L \nu_\tau) , & O_V^R &= (\bar{c}\gamma^\mu P_R b)(\bar{\tau}\gamma_\mu P_L \nu_\tau) , \\ O_S^R &= (\bar{c}P_R b)(\bar{\tau}P_L \nu_\tau) , & O_S^L &= (\bar{c}P_L b)(\bar{\tau}P_L \nu_\tau) , & O_T &= (\bar{c}\sigma^{\mu\nu} P_L b)(\bar{\tau}\sigma_{\mu\nu} P_L \nu_\tau) . \end{aligned} \quad (34)$$

Here the SM contribution has been factored out, so that $C_{V,S,T}^{L,R}$ are generated only through NP.

As was the case in the $b \rightarrow s\ell^+\ell^-$ EFT analysis, these operators are defined in the WET. In order to make contact with the NP that generates them, they must be mapped onto SMEFT. It turns out that all of these dimension-6 WET operators are also dimension-6 SMEFT operators, with one exception: O_V^R . An LFU version of this operator appears in SMEFT at dimension-6, but the LFUV operator shown above arises only at dimension 8 [137], so that its coefficient C_V^R is expected to be smaller than the other coefficients by $O(v^2/\Lambda^2)$, where v is the vev of the SM Higgs and Λ is the scale of NP. For this reason, O_V^R is usually excluded from EFT analyses. (For an alternative point of view, see Refs. [138?].)

The most recent EFT analysis of the $b \rightarrow c\tau^-\bar{\nu}_\tau$ anomalies was performed in Ref. [139]. This study used the five observables of Eqs. (29) and (31), and added $\mathcal{B}(B_c \rightarrow \tau\nu_\tau)$, assuming upper limits of 60%, 30% and 10%. The results are shown in Table 6. Note that tensor operators are generally generated by Fierz transformations. For example, the exchange of the scalar $SU(2)_L$ -doublet LQ R_2 produces the four-fermion operator $(\bar{c}P_L \nu_\tau)(\bar{\tau}P_L b)$ [140, 141]. A Fierz transformation produces both O_S^L and O_T , with $C_S^L = 4C_T$. This is used in the fits.

From this Table, we make the following observations:

- Among the 1D hypotheses, only a nonzero C_V^L provides a good explanation of the data.
- There are four 2D hypotheses that are good fits. Two of them – $(C_V^L, C_S^L = 4C_T)$ and (C_V^L, C_S^R) – are basically just the 1D best fit, with a small additional WC added. The goodness-of-fit of the other two – (C_S^R, C_S^L) and $(\text{Re}[C_S^L = 4C_T], \text{Im}[C_S^L = 4C_T])$ – depends critically on the upper limit of $\mathcal{B}(B_c \rightarrow \tau\nu_\tau)$. If this upper limit is 30% or 60%, these 2D hypotheses are viable. However, if the upper limit is 10%, these scenarios are disfavoured.
- We note that the difference between p values of 30% and 75% is not statistically significant – both describe perfectly acceptable fits. In fact, from a statistical point

¹⁶As discussed above, here we assume lepton flavour conservation. For an EFT analysis of $b \rightarrow c\ell^-\bar{\nu}_\ell$ and $b \rightarrow u\ell^-\bar{\nu}_\ell$ decays without LFC, see Ref. [136].

1D hypothesis	Best fit	p value (%)	Pull _{SM}
C_V^L	0.07 ± 0.02	44	4.0
C_S^R	0.09 ± 0.03	2.7	3.1
C_S^L	0.07 ± 0.03	0.26	2.1
$C_S^L = 4C_T$	-0.03 ± 0.04	0.04	0.7

2D hypothesis	Best fit	p value (%)	Pull _{SM}
$(C_V^L, C_S^L = 4C_T)$	$(0.10, -0.04)$	29.8	3.6
$(C_S^R, C_S^L) _{60\%}$	$(0.29, -0.25)$ $(-0.16, -0.69)$	75.7	3.9
$(C_S^R, C_S^L) _{30\%}$	$(0.21, -0.15)$ $(-0.26, -0.61)$	30.9	3.6
$(C_S^R, C_S^L) _{10\%}$	$(0.11, -0.04)$ $(-0.37, -0.51)$	2.6	2.9
(C_V^L, C_S^R)	$(0.08, 0.01)$	26.6	3.6
$(\text{Re}[C_S^L = 4C_T], \text{Im}[C_S^L = 4C_T]) _{60,30\%}$	$(-0.06, \pm 0.31)$	25.0	3.6
$(\text{Re}[C_S^L = 4C_T], \text{Im}[C_S^L = 4C_T]) _{10\%}$	$(-0.03, \pm 0.24)$	5.9	3.2

Table 6: Results of the one-dimensional and two-dimensional fits for the WCs (given at the matching scale of 1 TeV), including the five observables of Eqs. (29) and (31), with $\mathcal{B}(B_c \rightarrow \tau\nu_\tau) < 60\%$, 30% and 10% . For those entries without a label indicating the constraint on $\mathcal{B}(B_c \rightarrow \tau\nu_\tau)$, the fit is valid for all three upper limits. For the SM, the p -value is $\sim 0.1\%$, which represents a discrepancy with the data of 3.3σ .

of view, we expect the true solution to have a p value of $\sim 50\%$. Larger p values describe fits that are “too good,” and suggest that errors may be overestimated. In this sense, it may be that allowing $\mathcal{B}(B_c \rightarrow \tau\nu_\tau)$ to be as large as 60% is a bit too weak of a constraint. (Of course, this discussion will become moot with an actual measurement of $\mathcal{B}(B_c \rightarrow \tau\nu_\tau)$.)

4.3 Model analysis

When the $R_{D^{(*)}}$ anomalies were first announced, there were several different general EFT analyses that identified the WCs that could be modified in order to explain the data [142, 143, 144, 145]. Although they were model-independent, they did indicate what types of NP models should be considered. The key point is that $b \rightarrow c\tau^-\bar{\nu}_\tau$ is a charged-current process. Given that it is produced at tree level in the SM, the simplest models involve the tree-level exchange of a W' , a LQ, or a charged Higgs. We discuss these possibilities in turn, often within the context of the above EFT results.

4.3.1 W'

For the $b \rightarrow c\tau^-\bar{\nu}_\tau$ anomaly, the W' solution most often proposed involves a RH W_R , along with a light RH neutrino [146, 147, 148, 149]. A recent complete analysis can be found in Ref. [150]. A generic W' model, with arbitrary LH and RH couplings to both quarks and leptons, is examined in Ref. [151].

4.3.2 LQ models

The first paper to examine LQ models as a possible explanation of the $b \rightarrow c\tau^-\bar{\nu}_\tau$ anomaly is Ref. [118]. Followup papers can be found in Refs. [152, 153, 154, 155]. At present, the S_1 , U_1 and R_2 LQs [see Eq. (28)] can be viable explanations. The exchange of an S_1 or U_1 leads to a four-fermion operator that is equivalent to O_V^L of Eq. (34). As for R_2 , as mentioned above, its exchange leads to O_S^L and O_T , with $C_S^L = 4C_T$. So it can provide an explanation only for large values of $\mathcal{B}(B_c \rightarrow \tau\nu_\tau)$.

4.3.3 Charged Higgs

Another way of explaining the $b \rightarrow c\tau^-\bar{\nu}_\tau$ anomaly is through the tree-level exchange of a charged Higgs boson, and here numerous two-Higgs-doublet models (2HDMs) have been proposed [156, 157, 158, 159, 160, 161, 162, 163, 164, 165]. However, charged-Higgs exchange produces only O_S^R and O_S^L of Eq. (34), and as we saw in the EFT analysis, this solution is only viable if $\mathcal{B}(B_c \rightarrow \tau\nu_\tau)$ is large. In addition, there are strong constraints on the charged Higgs from the LHC [166].

A variety of measurements have been proposed to distinguish among the NP explanations. These include the q^2 distribution [167], D^* polarization [168, 169], τ polarizations [170], and the full angular distribution [171].

5 Links between the $b \rightarrow s\mu^+\mu^-$ and $b \rightarrow c\tau^-\bar{\nu}_\tau$ anomalies

5.1 SMEFT analysis

It was first shown in Ref. [172] that it is possible to simultaneously explain the $b \rightarrow s\mu^+\mu^-$ and $b \rightarrow c\tau^-\bar{\nu}_\tau$ anomalies. At that time (2014), it was thought that NP with purely LH couplings was required to account for the $b \rightarrow s\mu^+\mu^-$ data [119]. Referring to Eq. (16), we see that there are two SMEFT operators of this type:

$$\mathcal{O}_{ijkl}^{(1)} = (\bar{L}_i\gamma_\mu L_j)(\bar{Q}_k\gamma^\mu Q_l) \quad , \quad \mathcal{O}_{ijkl}^{(3)} = (\bar{L}_i\gamma_\mu\sigma^I L_j)(\bar{Q}_k\gamma^\mu\sigma^I Q_l) \quad , \quad (35)$$

where we have included the flavour indices in the names of the operators.

The key point is that, while $\mathcal{O}_{ijkl}^{(1)}$ is purely neutral current, $\mathcal{O}_{ijkl}^{(3)}$ contains both neutral-current and charged-current contributions. Thus, $\mathcal{O}_{2223}^{(1,3)}$ generate $b \rightarrow s\mu^+\mu^-$, $\mathcal{O}_{3323}^{(3)}$ produces $b \rightarrow c\tau^-\bar{\nu}_\tau$. The original idea of Ref. [172] (see also Refs. [173, 174]) was that the NP couples only (or mainly [173]) to the third generation in the gauge basis. Couplings

to the second generation are generated when one rotates to the mass basis. Since $\mathcal{O}_{2223}^{(1,3)}$ requires more such rotations than $\mathcal{O}_{3323}^{(3)}$, $\mathcal{C}_{2223}^{(1,3)}$ is naturally smaller than $\mathcal{C}_{3323}^{(3)}$. This is what is required since $b \rightarrow s\mu^+\mu^-$ is loop level in the SM, while $b \rightarrow c\tau^-\bar{\nu}_\tau$ is tree level. In Ref. [175], it was shown that, even if one makes no assumptions about the coupling of the NP in the gauge basis, when all constraints are taken into account, one finds the same pattern as above for the WCs. Thus, both B anomalies can be explained simultaneously if the NP is purely LH and generates $\mathcal{O}_{ijkl}^{(1)}$ and $\mathcal{O}_{ijkl}^{(3)}$.

But there's more. In addition to producing $b \rightarrow c\tau^-\bar{\nu}_\tau$, $\mathcal{O}_{3323}^{(3)}$ also generates $b \rightarrow s\tau^+\tau^-$ [63]. This has two effects. First, it implies that the branching ratios of decays governed by $b \rightarrow s\tau^+\tau^-$ should be much larger than what is predicted by the SM. Second, this coupling is precisely what is required to produce \mathcal{C}_9^U in $b \rightarrow s\mu^+\mu^-$ at one loop (see Sec. 3.3.2).

Thus, this combined explanation of the two B anomalies reproduces the favoured $[\mathcal{C}_9^V = -\mathcal{C}_{10}^V, \mathcal{C}_9^U]$ solution (see Eq. (11)) of the $b \rightarrow s\mu^+\mu^-$ anomalies. The combined Pull_{SM} of this particular scenario is as high as 8.1σ . The central values found for the WCs in this case are $\mathcal{C}_9^V = -\mathcal{C}_{10}^V = -0.36, \mathcal{C}_9^U = -0.74$ [49].

5.2 Model analysis

As shown above, it is possible to find a combined explanation of the $b \rightarrow s\mu^+\mu^-$ and $b \rightarrow c\tau^-\bar{\nu}_\tau$ anomalies if the NP generates the operators $\mathcal{O}_{ijkl}^{(1)}$ and $\mathcal{O}_{ijkl}^{(3)}$. That is, the NP must couple to LH particles and have the appropriate couplings to produce $b \rightarrow s\mu^+\mu^-$ and $b \rightarrow c\tau^-\bar{\nu}_\tau$.

Now, in an EFT analysis, one can focus on a particular operator. However, in a model, additional operators will generally be produced, and these lead to additional constraints. Thus, in order to test whether a particular model is viable, one must consider all of these constraints.

5.2.1 VB (W', Z') models

The vector-boson (VB) model, which contains a SM-like $SU(2)_L$ triplet of vector bosons (W', Z'), can potentially provide a simultaneous explanation of both B anomalies. The Z' and W' respectively mediate the $b \rightarrow s\mu^+\mu^-$ and $b \rightarrow c\tau^-\bar{\nu}_\tau$ transitions, and their couplings can be chosen to reproduce the experimental data. Explicit VB models have been proposed in Refs. [173, 176].

On the other hand, there are additional constraints on the VB model. These include the constraints on the Z' couplings described in Sec. 3.6.1, but there are also constraints from lepton-flavour-violating processes. The VB model has been examined in detail in Refs. [175, 177, 178]. There it is found that, when all the constraints are taken into account, the VB model is excluded as a simultaneous explanation of both anomalies.

5.2.2 LQ models

1. Single-LQ solutions: Over the years, many single-LQ solutions were proposed as a simultaneous solution of the $b \rightarrow s\mu^+\mu^-$ and $b \rightarrow c\tau^-\bar{\nu}_\tau$ anomalies. As new data appeared, certain solutions were ruled out. The combined EFT analysis in Ref. [178] clearly demonstrated that the only viable single-LQ solution is the one based on the vector LQ U_1 , which was first discussed in Refs. [26, 174, 179]. This conclusion was further confirmed in Ref. [180], which considered all single-LQ solutions, taking into account LHC constraints.
2. Two-LQ solutions: In Ref. [181], it is proposed to simultaneously explain the anomalies with the addition of two scalar LQs, S_1 and S_3 . S_3 contributes to both $b \rightarrow s\mu^+\mu^-$ and $b \rightarrow c\tau^-\bar{\nu}_\tau$, but it cannot explain both anomalies by itself. S_1 contributes to $b \rightarrow c\tau^-\bar{\nu}_\tau$, but not $b \rightarrow s\mu^+\mu^-$. And both LQs contribute to $b \rightarrow s\nu\bar{\nu}$. It is possible to choose the couplings of S_1 and S_3 such that both anomalies are explained, while evading the constraints from $b \rightarrow s\nu\bar{\nu}$.

5.2.3 UV Completions

The idea of explaining both anomalies with a single NP particle is very intriguing, so the U_1 solution has generated a great deal of interest. One problem with this solution is that, since the U_1 is a vector LQ, the theory with a U_1 , but without a Higgs sector, is not renormalizable. As a consequence, loop diagrams, which can lead to potentially important effects, cannot be calculated. In order to address this problem, a number of papers have constructed models with an extended gauge group that is broken at the TeV scale and contains the U_1 LQ as a gauge boson, or as a composite state. A key observation, made first in Ref. [179], is that the U_1 field points to a unification of quarks and leptons via a local or global $SU(4)$ symmetry.

These UV completion models can be split into two categories. First, there are the models that use variations of the Pati-Salam idea, in which $SU(4)_{PS}$ unifies $SU(3)_C$ and a $U(1)$ under which both quarks and leptons are charged (e.g., $U(1)_Y$ or $U(1)_{B-L}$) [182, 183, 184, 185, 186, 187, 188, 189, 190, 191, 192, 193]. Second, some models use the “4321” gauge group, $SU(4) \times SU(3)' \times SU(2)_L \times U(1)_X$ [194, 195, 196]. In all cases, it must be ensured that the breaking of the gauge group at the TeV scale does not run into any problems from low-energy flavour constraints.

6 Connections with other physics problems

There are several other experimental results that cannot be explained by the SM. If NP is present, its effects could possibly be seen in different types of observables. With this in mind, models have been proposed that simultaneously explain the B anomalies and (at least) one of these other discrepancies with the SM. Below we discuss models that relate the B anomalies (mostly $b \rightarrow s\ell^+\ell^-$) to dark matter, $(g-2)_\mu$, neutrino masses, and hadronic anomalies. But there are also attempts to make connections with other

observables that exhibit tensions with the SM, such as the Cabibbo angle anomaly, the $Z \rightarrow \bar{b}b$ forward-backward asymmetry, and $\tau \rightarrow \mu\bar{\nu}\nu$, see Ref. [197] for example.

6.1 Dark matter

There is considerable cosmological and astrophysical evidence supporting the existence of dark matter (DM). However, the fact that the SM has no DM candidate is another one of its shortcomings, and provides another reason for the requirement of NP. A number of papers have explored possible links between these two strong hints of NP, the $b \rightarrow s\ell^+\ell^-$ anomalies and DM. In Ref. [198], these models are separated into two categories: (i) portal models, in which the relic density mediator is the same as that in the B anomalies, and (ii) loop models, in which the $b \rightarrow s\ell^+\ell^-$ anomalies are explained via loops that include DM. In the discussion of $b \rightarrow s\ell^+\ell^-$ models in Sec. 3.6, we elected to focus only on the simplest models. These include only models of type (i); models of type (ii) contain many more particles, are subject to more constraints, and are often valid only in a corner of parameter space. Portal models with a Z' mediator can be found in Refs. [72, 74, 75, 77, 79, 80, 82, 94, 95, 96, 97, 102, 199]. (These do not include models in which the Z' is allowed to decay to DM in order to evade LHC constraints, but do not otherwise address the DM issues of relic density and direct detection.) Refs. [124, 196, 200, 201], which include combined explanations of both the $b \rightarrow s\ell^+\ell^-$ and $b \rightarrow c\ell^-\bar{\nu}_\ell$ anomalies, describe portal models with LQs.

6.2 $(g - 2)_\mu$

Recently, the Muon $g - 2$ Collaboration released a new result: the measurement of $a_\mu \equiv (g - 2)_\mu/2$ disagrees with the SM prediction by 4.2σ [202]. Following this announcement, a number of papers were written proposing models to simultaneously explain the observed value of a_μ and one or both of the B anomalies. There are many different scenarios, but all of them use a Z' and/or LQs, see Refs. [115, 116, 203, 204, 205, 206, 207, 208, 209, 210, 211].

6.3 Neutrino properties

Another weakness of the SM is that it has no explanation for neutrino masses. Here too, models have been proposed that provide combined explanations of the B anomalies and neutrino masses. However, it must be said that the connection between the two is usually rather tenuous in these models, and they generally involve several different types of NP particles. See Refs. [212, 213, 214, 215] for recent examples of such models.

6.4 Hadronic anomalies

The $b \rightarrow s\ell^+\ell^-$ and $b \rightarrow c\ell^-\bar{\nu}_\ell$ anomalies both involve semileptonic transitions. However, there is also some tension with the SM in certain purely hadronic B decays, albeit at a much lower level. Attempts have been made to link the semileptonic and hadronic anomalies.

For many years, the measurements of the branching ratios and direct & indirect CP asymmetries in $B \rightarrow \pi K$ decays ($B^0 \rightarrow \pi^- K^+$, $B^0 \rightarrow \pi^0 K^0$, $B^+ \rightarrow \pi^0 K^+$, $B^+ \rightarrow \pi^+ K^0$) have exhibited a slight inconsistency. This can be ameliorated if there is a NP contribution to the $b \rightarrow s$ electroweak penguin. In Ref. [216], an update of the “ $B \rightarrow \pi K$ puzzle” was performed, and it was noted that this could be explained if the Z' used to explain the $b \rightarrow s\mu^+\mu^-$ anomaly also couples to RH $u\bar{u}$ and/or $d\bar{d}$, with unequal couplings.

U spin is an approximate symmetry that treats d and s quarks as identical. Under U spin, the two transitions $b \rightarrow s$ and $b \rightarrow d$ are equal, apart from CKM matrix elements. Note that these two amplitudes involve second-generation and first-generation *quarks* in the final state. A certain parallel may be drawn with $b \rightarrow s\mu^+\mu^-$ and $b \rightarrow se^+e^-$, which involve second-generation and first-generation *leptons* in the final state. In the latter case, the ratio of the two amplitudes tests LFUV (involving QED), while in the former it measures U-spin breaking (involving QCD). This shows the limitations of the analogy.

Inspired by this observation, the authors of Ref. [218] constructed an optimized observable, $L_{K^*\bar{K}^*}$, from the ratio of longitudinal amplitudes for $B_s \rightarrow \bar{K}^{0*}K^{0*}$ ($b \rightarrow s$) and $B_d \rightarrow \bar{K}^{0*}K^{0*}$ ($b \rightarrow d$) that can be predicted (in contrast to the other amplitudes in which infrared-divergences enter at leading order). The results were as follows:

- The U-spin breaking in the ratio was computed within the SM using QCDF and modeling power-suppressed but infrared-divergent weak annihilation and hard-spectator scattering. Taking this into account, there is a tension with the SM at the level of 2.6σ in $L_{K^*\bar{K}^*}$.
- The $b \rightarrow s$ amplitude is smaller than the $b \rightarrow d$ amplitude in the same way as there is a deficit in $b \rightarrow s\mu^+\mu^-$ as compared to $b \rightarrow se^+e^-$.
- There is a dominant operator that can naturally explain the low value of $L_{K^*\bar{K}^*}$ as it happens for $b \rightarrow s\ell\ell$ with O_9 . The Wilson coefficient of this dominant operator also gets a destructive NP contribution with a $\sim 20\%$ of the SM size.
- A possible connection with the $b \rightarrow s\ell\ell$ anomalies is to consider a composite/extra-dimensional model whose particle spectrum includes a Kaluza-Klein gluon and a Z' .

7 An EFT glance into the future

The future prospects for the field of B flavour anomalies are very exciting – we expect a plethora of new data and updates of previous measurements. Indeed, in the coming five years, the search for NP using these anomalies is expected to play a leading role at CERN and particularly at Belle-II.

7.1 $b \rightarrow s\mu^+\mu^-$ anomalies

In the very near future, we expect to receive two different types of input:

- LFUV observables. In the short term, measurements of R_{K_S} , $R_{K^{*+}}$ (based on the charged channel $B^+ \rightarrow K^{*+}\ell^+\ell^-$) and R_ϕ (based upon $B_s \rightarrow \phi\ell\ell$) are expected from LHCb. These results will test whether or not there is LFUV in Nature, which is what the present measurements of R_{K^*} and especially R_K are clearly pointing to. In the medium term, once more data is accumulated, an update of the observable R_K , possibly increasing its significance much beyond the present evidence for NP, will be a crucial milestone.
- Angular optimized observables. Here we can expect updates of the optimized observables of the 4-body angular distributions of $B_d^0 \rightarrow K^*(\rightarrow K\pi)\mu^+\mu^-$ (the last update was in 2020 [217]), the corresponding B^+ decay, and $B_s^0 \rightarrow \phi(\rightarrow K^+K^-)\mu^+\mu^-$. All of these will be important, but the first one will be particularly interesting, to see if the first anomaly, that is the observable P'_5 , increases with more data.

In addition, an important next step in this program will be the study of the angular observables entering the S -wave part of the $B \rightarrow K\pi\ell^+\ell^-$ decay. These new S -wave observables will provide complementary information to the P -wave part of the distribution [219].

Finally, at present, the two scenarios with the largest Pull_{SM} are the 2D hypotheses $[\mathcal{C}_{9\mu}^{\text{NP}}, \mathcal{C}'_{9\mu}{}^{\text{NP}} = -\mathcal{C}'_{10\mu}{}^{\text{NP}}]$ and $[\mathcal{C}_9^V = -\mathcal{C}_{10}^V, \mathcal{C}_9^U]$ (Eq. (12)). It will be interesting to see which of these dominates as the preferred explanation, or if another solution emerges. It was shown in Refs. [38, 49, 220] that, while R_K and R_{K^*} cannot disentangle between these two scenarios, a precise measurement of the observable Q_5 in the bin $[1.1, 6]$ GeV^2 can separate them, with $Q_5 \sim 0.08$ for the second scenario, and $Q_5 \sim 0.32$ for the first.

7.2 $b \rightarrow c\tau^-\bar{\nu}_\tau$ anomalies

At the end of Sec. 4.3, we note that a variety of measurements have been proposed to distinguish among the NP explanations. There is one that is particularly promising: it can, in principle, pinpoint what type of NP is present. Ref. [171] proposes measuring the angular distribution in $\bar{B} \rightarrow D^*(\rightarrow D\pi')\tau^-(\rightarrow \pi^-\nu_\tau)\bar{\nu}_\tau$. By measuring the four-momenta of the final-state D , π' and π^- , the differential decay rate can be constructed. This depends on two non-angular variables, q^2 and E_π , and three angles. Here, q^2 is the invariant mass-squared of the $\tau^-\bar{\nu}_\tau$ pair and E_π is the energy of the π^- in the τ decay. The idea is then to separate the data into various q^2 - E_π bins, and then to perform an angular analysis within each bin. The angular distribution consists of twelve different angular functions; nine of these are CP-conserving, and three are CP-violating. We therefore potentially have a large number of observables in this differential decay rate; the exact number depends on how many q^2 - E_π bins there are.

In the angular distributions, the coefficients of each angular function are functions of q^2 , E_π , and the NP coefficients of Eq. (34). There are five NP operators; only one linear combination of the two scalar operators contributes to the decay ($O_S^L + O_S^R$ does not). With complex coefficients, there are eight unknown theoretical parameters. Thus, if the angular distribution in $\bar{B} \rightarrow D^*(\rightarrow D\pi')\tau^-(\rightarrow \pi^-\nu_\tau)\bar{\nu}_\tau$ can be measured, it may be

possible to extract all of the NP coefficients from a fit, thus revealing what type of NP is present.

8 Summary

Despite its enormous success, the SM of particle physics is not complete – there must exist physics beyond the SM. Direct searches at the LHC for this new physics have thus far proven fruitless. On the other hand, there are deviations from the predictions of the SM in a number of observables involving $b \rightarrow s\ell^+\ell^-$ and $b \rightarrow c\ell^-\bar{\nu}_\ell$ decays. These are the B flavour anomalies, and they provide an indirect hint of NP.

The $b \rightarrow s\ell^+\ell^-$ anomalies have been seen in a number of different observables, measured by different experimental groups. At present, the p-value of the SM fit to all the $b \rightarrow s\ell\ell$ data is $\sim 1.1\%$, corresponding to a discrepancy with the data of $\sim 2.5\sigma$. Global fits to the data have been performed by different groups. Despite having different methodologies, the results are remarkably consistent, particularly between the ACDMN and HMMN groups. Using the results of the ACDMN group [49], the preferred 1D solutions are $\mathcal{C}_{9\mu}^{\text{NP}}$ ($\text{Pull}_{\text{SM}} = 7.0\sigma$) and $\mathcal{C}_{9\mu}^{\text{NP}} = -\mathcal{C}_{10\mu}^{\text{NP}}$ (6.2σ), and the preferred 2D solutions are $[\mathcal{C}_{9\mu}^{\text{NP}}, \mathcal{C}_{9\mu}^{\text{NP}} = -\mathcal{C}_{10\mu}^{\text{NP}}]$ (7.4σ) and $[\mathcal{C}_9^V = -\mathcal{C}_{10}^V, \mathcal{C}_9^U]$ (7.3σ). The simplest models involve the tree-level exchange of a Z' or a LQ.

The $b \rightarrow c\ell^-\bar{\nu}_\ell$ anomalies have been seen in fewer observables than $b \rightarrow s\ell^+\ell^-$, but here too, they have been measured by different experiments, with the results largely confirmed. The p-value of the SM fit to the present data is $\sim 0.1\%$, corresponding to a discrepancy of 3.3σ . The question of the identification of the underlying NP is complicated by the fact that we do not know if the neutrino is LH or RH. Assuming a LH neutrino, the preferred solution in the global fit is C_V^L i.e., LH NP, with $\text{Pull}_{\text{SM}} = 4.0\sigma$. Models involve the tree-level exchange of a W' or a LQ. If $\mathcal{B}(B_c \rightarrow \tau\nu_\tau)$ is allowed to be as large as 60%, (C_S^R, C_S^L) , i.e., scalar NP such as a charged Higgs, also provides a good solution.

It is obviously far too early to bet on a particular NP explanation, but one intriguing possibility is the vector LQ U_1 . It can simultaneously explain both anomalies, and in the case of $b \rightarrow s\ell^+\ell^-$, it can generate one of the preferred solutions, $[\mathcal{C}_9^V = -\mathcal{C}_{10}^V, \mathcal{C}_9^U]$.

These are exciting times. We may be seeing indirect evidence of NP at low energies. In the near future, LHCb and especially Belle II will produce new results. These will include measurements of previously-measured quantities, as well as new ones, such as Q_5 , observables involving $b \rightarrow s\tau^+\tau^-$, and $\mathcal{B}(B_c \rightarrow \tau\nu_\tau)$. All of this information will give us a better idea of what the underlying NP is.

Note added: As this review was being finalized, the measurements of R_{K_S} and $R_{K^{*+}}$ were reported by LHCb [221]. R_{K_S} was measured in the bin $[1.1, 6]$ GeV², while $R_{K^{*+}}$ was measured in a wider bin, $[0.045, 6.0]$ GeV², and exhibit tensions with the SM of 1.5σ and 1.4σ , respectively. These are not large disagreements, but they are in the same direction as previous measurements, and reinforce the case for LFUV.

Disclosure Statement: The authors are not aware of any affiliations, memberships, funding, or financial holdings that might be perceived as affecting the objectivity of this review.

Acknowledgments: We would like to acknowledge useful discussions with Andreas Crivellin, Gino Isidori, Avelino Vicente and Nazila Mahmoudi. The work of DL was partially financially supported by NSERC of Canada. This work received financial support from the Spanish Ministry of Science, Innovation and Universities (FPA2017-86989-P) and the Research Grant Agency of the Government of Catalonia (SGR 1069) [JM]. JM acknowledges the financial support by ICREA under the ICREA Academia programme.

References

- [1] R. Aaij *et al.* [LHCb], “Measurement of Form-Factor-Independent Observables in the Decay $B^0 \rightarrow K^{*0}\mu^+\mu^-$,” *Phys. Rev. Lett.* **111** (2013), 191801 doi:10.1103/PhysRevLett.111.191801 [arXiv:1308.1707 [hep-ex]].
- [2] S. Descotes-Genon, J. Matias, M. Ramon and J. Virto, “Implications from clean observables for the binned analysis of $B^- \rightarrow K^* \mu^+ \mu^-$ at large recoil,” *JHEP* **01** (2013), 048 doi:10.1007/JHEP01(2013)048 [arXiv:1207.2753 [hep-ph]].
- [3] S. Descotes-Genon, J. Matias and J. Virto, “Understanding the $B \rightarrow K^* \mu^+ \mu^-$ Anomaly,” *Phys. Rev. D* **88** (2013), 074002 doi:10.1103/PhysRevD.88.074002 [arXiv:1307.5683 [hep-ph]].
- [4] R. Aaij *et al.* [LHCb], “Test of lepton universality using $B^+ \rightarrow K^+ \ell^+ \ell^-$ decays,” *Phys. Rev. Lett.* **113**, 151601 (2014) doi:10.1103/PhysRevLett.113.151601 [arXiv:1406.6482 [hep-ex]].
- [5] G. Hiller and F. Kruger, “More model-independent analysis of $b \rightarrow s$ processes,” *Phys. Rev. D* **69** (2004), 074020 doi:10.1103/PhysRevD.69.074020 [arXiv:hep-ph/0310219 [hep-ph]].
- [6] J. P. Lees *et al.* [BaBar], “Evidence for an excess of $\bar{B} \rightarrow D^{(*)} \tau^- \bar{\nu}_\tau$ decays,” *Phys. Rev. Lett.* **109**, 101802 (2012) doi:10.1103/PhysRevLett.109.101802 [arXiv:1205.5442 [hep-ex]].
- [7] J. P. Lees *et al.* [BaBar], “Measurement of an Excess of $\bar{B} \rightarrow D^{(*)} \tau^- \bar{\nu}_\tau$ Decays and Implications for Charged Higgs Bosons,” *Phys. Rev. D* **88**, no.7, 072012 (2013) doi:10.1103/PhysRevD.88.072012 [arXiv:1303.0571 [hep-ex]].
- [8] M. Huschle *et al.* [Belle], “Measurement of the branching ratio of $\bar{B} \rightarrow D^{(*)} \tau^- \bar{\nu}_\tau$ relative to $\bar{B} \rightarrow D^{(*)} \ell^- \bar{\nu}_\ell$ decays with hadronic tagging at Belle,” *Phys. Rev. D* **92**, no.7, 072014 (2015) doi:10.1103/PhysRevD.92.072014 [arXiv:1507.03233 [hep-ex]].

- [9] R. Aaij *et al.* [LHCb], “Measurement of the ratio of branching fractions $\mathcal{B}(\bar{B}^0 \rightarrow D^{*+}\tau^-\bar{\nu}_\tau)/\mathcal{B}(\bar{B}^0 \rightarrow D^{*+}\mu^-\bar{\nu}_\mu)$,” Phys. Rev. Lett. **115**, no.11, 111803 (2015) [erratum: Phys. Rev. Lett. **115**, no.15, 159901 (2015)] doi:10.1103/PhysRevLett.115.111803 [arXiv:1506.08614 [hep-ex]].
- [10] F. Kruger and J. Matias, “Probing new physics via the transverse amplitudes of $B^0 \rightarrow K^{*0}(\rightarrow K^-\pi^+)l^+l^-$ at large recoil,” Phys. Rev. D **71** (2005), 094009 doi:10.1103/PhysRevD.71.094009 [arXiv:hep-ph/0502060 [hep-ph]].
- [11] W. Altmannshofer, P. Ball, A. Bharucha, A. J. Buras, D. M. Straub and M. Wick, “Symmetries and Asymmetries of $B \rightarrow K^*\mu^+\mu^-$ Decays in the Standard Model and Beyond,” JHEP **01** (2009), 019 doi:10.1088/1126-6708/2009/01/019 [arXiv:0811.1214 [hep-ph]].
- [12] D. Becirevic and E. Schneider, “On transverse asymmetries in $B \rightarrow K^*l^+l^-$,” Nucl. Phys. B **854** (2012), 321-339 doi:10.1016/j.nuclphysb.2011.09.004 [arXiv:1106.3283 [hep-ph]].
- [13] J. Matias, F. Mescia, M. Ramon and J. Virto, “Complete Anatomy of $\bar{B}_{d-} \rightarrow \bar{K}^{*0}(\rightarrow K\pi)l^+l^-$ and its angular distribution,” JHEP **04** (2012), 104 doi:10.1007/JHEP04(2012)104 [arXiv:1202.4266 [hep-ph]].
- [14] S. Descotes-Genon, T. Hurth, J. Matias and J. Virto, “Optimizing the basis of $B \rightarrow K^*ll$ observables in the full kinematic range,” JHEP **05** (2013), 137 doi:10.1007/JHEP05(2013)137 [arXiv:1303.5794 [hep-ph]].
- [15] J. Gratrex, M. Hopfer and R. Zwicky, “Generalised helicity formalism, higher moments and the $B \rightarrow K_{J_K}(\rightarrow K\pi)\bar{\ell}_1\ell_2$ angular distributions,” Phys. Rev. D **93** (2016) no.5, 054008 doi:10.1103/PhysRevD.93.054008 [arXiv:1506.03970 [hep-ph]].
- [16] M. Bordone, G. Isidori and A. Pattori, “On the Standard Model predictions for R_K and R_{K^*} ,” Eur. Phys. J. C **76** (2016) no.8, 440 doi:10.1140/epjc/s10052-016-4274-7 [arXiv:1605.07633 [hep-ph]].
- [17] G. Isidori, S. Nabeebaccus and R. Zwicky, “QED corrections in $\bar{B} \rightarrow \bar{K}\ell^+\ell^-$ at the double-differential level,” JHEP **12** (2020), 104 doi:10.1007/JHEP12(2020)104 [arXiv:2009.00929 [hep-ph]].
- [18] R. Aaij *et al.* [LHCb], “Test of lepton universality in beauty-quark decays,” [arXiv:2103.11769 [hep-ex]].
- [19] R. Aaij *et al.* [LHCb], “Test of lepton universality with $B^0 \rightarrow K^{*0}\ell^+\ell^-$ decays,” JHEP **08** (2017), 055 doi:10.1007/JHEP08(2017)055 [arXiv:1705.05802 [hep-ex]].
- [20] S. Choudhury *et al.* [BELLE], “Test of lepton flavor universality and search for lepton flavor violation in $B \rightarrow K\ell\ell$ decays,” JHEP **03** (2021), 105 doi:10.1007/JHEP03(2021)105 [arXiv:1908.01848 [hep-ex]].

- [21] A. Abdesselam *et al.* [Belle], “Test of Lepton-Flavor Universality in $B \rightarrow K^* \ell^+ \ell^-$ Decays at Belle,” *Phys. Rev. Lett.* **126** (2021) no.16, 161801 doi:10.1103/PhysRevLett.126.161801 [arXiv:1904.02440 [hep-ex]].
- [22] B. Capdevila, S. Descotes-Genon, J. Matias and J. Virto, “Assessing lepton-flavour non-universality from $B \rightarrow K^* \ell \ell$ angular analyses,” *JHEP* **10** (2016), 075 doi:10.1007/JHEP10(2016)075 [arXiv:1605.03156 [hep-ph]].
- [23] S. Wehle *et al.* [Belle], “Lepton-Flavor-Dependent Angular Analysis of $B \rightarrow K^* \ell^+ \ell^-$,” *Phys. Rev. Lett.* **118** (2017) no.11, 111801 doi:10.1103/PhysRevLett.118.111801 [arXiv:1612.05014 [hep-ex]].
- [24] U. Egede *et al.*, Annual Review of Particle Physics in preparation.
- [25] G. Buchalla, A. J. Buras and M. E. Lautenbacher, “Weak decays beyond leading logarithms,” *Rev. Mod. Phys.* **68** (1996), 1125-1144 doi:10.1103/RevModPhys.68.1125 [arXiv:hep-ph/9512380 [hep-ph]].
- [26] R. Alonso, B. Grinstein and J. Martin Camalich, “ $SU(2) \times U(1)$ gauge invariance and the shape of new physics in rare B decays,” *Phys. Rev. Lett.* **113**, 241802 (2014) doi:10.1103/PhysRevLett.113.241802 [arXiv:1407.7044 [hep-ph]].
- [27] T. Huber, E. Lunghi, M. Misiak and D. Wyler, “Electromagnetic logarithms in $\bar{B} \rightarrow X_s \ell^+ \ell^-$,” *Nucl. Phys. B* **740** (2006), 105-137 doi:10.1016/j.nuclphysb.2006.01.037 [arXiv:hep-ph/0512066 [hep-ph]].
- [28] P. Gambino, M. Gorbahn and U. Haisch, “Anomalous dimension matrix for radiative and rare semileptonic B decays up to three loops,” *Nucl. Phys. B* **673** (2003), 238-262 doi:10.1016/j.nuclphysb.2003.09.024 [arXiv:hep-ph/0306079 [hep-ph]].
- [29] C. Bobeth, P. Gambino, M. Gorbahn and U. Haisch, “Complete NNLO QCD analysis of anti-B \rightarrow X(s) $\ell^+ \ell^-$ and higher order electroweak effects,” *JHEP* **04** (2004), 071 doi:10.1088/1126-6708/2004/04/071 [arXiv:hep-ph/0312090 [hep-ph]].
- [30] M. Misiak and M. Steinhauser, “NNLO QCD corrections to the anti-B \rightarrow X(s) gamma matrix elements using interpolation in $m(c)$,” *Nucl. Phys. B* **764** (2007), 62-82 doi:10.1016/j.nuclphysb.2006.11.027 [arXiv:hep-ph/0609241 [hep-ph]].
- [31] T. Huber, T. Hurth and E. Lunghi, “Logarithmically Enhanced Corrections to the Decay Rate and Forward Backward Asymmetry in $\bar{B} \rightarrow X_s \ell^+ \ell^-$,” *Nucl. Phys. B* **802** (2008), 40-62 doi:10.1016/j.nuclphysb.2008.04.028 [arXiv:0712.3009 [hep-ph]].
- [32] K. Kowalska, D. Kumar and E. M. Sessolo, “Implications for new physics in $b \rightarrow s \mu \mu$ transitions after recent measurements by Belle and LHCb,” *Eur. Phys. J. C* **79** (2019) no.10, 840 doi:10.1140/epjc/s10052-019-7330-2 [arXiv:1903.10932 [hep-ph]].

- [33] T. Blake, S. Meinel and D. van Dyk, “Bayesian Analysis of $b \rightarrow s\mu^+\mu^-$ Wilson Coefficients using the Full Angular Distribution of $\Lambda_b \rightarrow \Lambda(\rightarrow p\pi^-)\mu^+\mu^-$ Decays,” *Phys. Rev. D* **101** (2020) no.3, 035023 doi:10.1103/PhysRevD.101.035023 [arXiv:1912.05811 [hep-ph]].
- [34] M. Ciuchini, A. M. Coutinho, M. Fedele, E. Franco, A. Paul, L. Silvestrini and M. Valli, “On Flavourful Easter eggs for New Physics hunger and Lepton Flavour Universality violation,” *Eur. Phys. J. C* **77** (2017) no.10, 688 doi:10.1140/epjc/s10052-017-5270-2 [arXiv:1704.05447 [hep-ph]].
- [35] L. S. Geng, B. Grinstein, S. Jäger, S. Y. Li, J. Martin Camalich and R. X. Shi, “Implications of new evidence for lepton-universality violation in $b \rightarrow s\ell + \ell^-$ decays,” *Phys. Rev. D* **104** (2021) no.3, 035029 doi:10.1103/PhysRevD.104.035029 [arXiv:2103.12738 [hep-ph]].
- [36] C. Cornella, D. A. Faroughy, J. Fuentes-Martin, G. Isidori and M. Neubert, “Reading the footprints of the B-meson flavor anomalies,” *JHEP* **08**, 050 (2021) doi:10.1007/JHEP08(2021)050 [arXiv:2103.16558 [hep-ph]].
- [37] S. Descotes-Genon, L. Hofer, J. Matias and J. Virto, “Global analysis of $b \rightarrow s\ell\ell$ anomalies,” *JHEP* **06** (2016), 092 doi:10.1007/JHEP06(2016)092 [arXiv:1510.04239 [hep-ph]].
- [38] M. Algueró, B. Capdevila, A. Crivellin, S. Descotes-Genon, P. Masjuan, J. Matias, M. Novoa Brunet and J. Virto, “Emerging patterns of New Physics with and without Lepton Flavour Universal contributions,” *Eur. Phys. J. C* **79** (2019) no.8, 714 doi:10.1140/epjc/s10052-019-7216-3 [arXiv:1903.09578 [hep-ph]].
- [39] R. Aaij *et al.* [LHCb], “Differential branching fraction and angular analysis of $\Lambda_b^0 \rightarrow \Lambda\mu^+\mu^-$ decays,” *JHEP* **06** (2015), 115 [erratum: *JHEP* **09** (2018), 145] doi:10.1007/JHEP06(2015)115 [arXiv:1503.07138 [hep-ex]].
- [40] S. Descotes-Genon, L. Hofer, J. Matias and J. Virto, “On the impact of power corrections in the prediction of $B \rightarrow K^*\mu^+\mu^-$ observables,” *JHEP* **12** (2014), 125 doi:10.1007/JHEP12(2014)125 [arXiv:1407.8526 [hep-ph]].
- [41] B. Capdevila, S. Descotes-Genon, L. Hofer and J. Matias, “Hadronic uncertainties in $B \rightarrow K^*\mu^+\mu^-$: a state-of-the-art analysis,” *JHEP* **04** (2017), 016 doi:10.1007/JHEP04(2017)016 [arXiv:1701.08672 [hep-ph]].
- [42] A. Khodjamirian, T. Mannel, A. A. Pivovarov and Y. M. Wang, “Charm-loop effect in $B \rightarrow K^{(*)}\ell^+\ell^-$ and $B \rightarrow K^*\gamma$,” *JHEP* **09** (2010), 089 doi:10.1007/JHEP09(2010)089 [arXiv:1006.4945 [hep-ph]].
- [43] N. Gubernari, A. Kokulu and D. van Dyk, “ $B \rightarrow P$ and $B \rightarrow V$ Form Factors from B -Meson Light-Cone Sum Rules beyond Leading Twist,” *JHEP* **01** (2019), 150 doi:10.1007/JHEP01(2019)150 [arXiv:1811.00983 [hep-ph]].

- [44] A. Bharucha, D. M. Straub and R. Zwicky, “ $B \rightarrow V\ell^+\ell^-$ in the Standard Model from light-cone sum rules,” JHEP **08** (2016), 098 doi:10.1007/JHEP08(2016)098 [arXiv:1503.05534 [hep-ph]].
- [45] N. Gubernari, D. van Dyk and J. Virto, “Non-local matrix elements in $B_{(s)} \rightarrow \{K^{(*)}, \phi\}\ell^+\ell^-$,” JHEP **02** (2021), 088 doi:10.1007/JHEP02(2021)088 [arXiv:2011.09813 [hep-ph]].
- [46] T. Blake, U. Egede, P. Owen, K. A. Petridis and G. Pomery, “An empirical model to determine the hadronic resonance contributions to $\bar{B}^0 \rightarrow \bar{K}^{*0}\mu^+\mu^-$ transitions,” Eur. Phys. J. C **78** (2018) no.6, 453 doi:10.1140/epjc/s10052-018-5937-3 [arXiv:1709.03921 [hep-ph]].
- [47] C. Bobeth, M. Chrzaszcz, D. van Dyk and J. Virto, “Long-distance effects in $B \rightarrow K^*\ell\ell$ from analyticity,” Eur. Phys. J. C **78** (2018) no.6, 451 doi:10.1140/epjc/s10052-018-5918-6 [arXiv:1707.07305 [hep-ph]].
- [48] M. Beneke, T. Feldmann and D. Seidel, “Systematic approach to exclusive $B \rightarrow V\ell^+\ell^-$, $V\gamma$ decays,” Nucl. Phys. B **612** (2001), 25-58 doi:10.1016/S0550-3213(01)00366-2 [arXiv:hep-ph/0106067 [hep-ph]].
- [49] M. Algueró, B. Capdevila, S. Descotes-Genon, J. Matias and M. Novoa-Brunet, “ $b \rightarrow s\ell\ell$ global fits after Moriond 2021 results,” [arXiv:2104.08921 [hep-ph]].
- [50] W. Altmannshofer and P. Stangl, “New Physics in Rare B Decays after Moriond 2021,” [arXiv:2103.13370 [hep-ph]].
- [51] J. Matias and P. Stangl, “Status of Global Fits of Flavour Anomalies,” talk given at the *Beyond the Flavour Anomalies II* conference, IPPP, Durham, April 2021.
- [52] T. Hurth, F. Mahmoudi, D. Martinez Santos and S. Neshatpour, “More Indications for Lepton Nonuniversality in $b \rightarrow s\ell^+\ell^-$,” [arXiv:2104.10058 [hep-ph]].
- [53] B. Capdevila, A. Crivellin, S. Descotes-Genon, J. Matias and J. Virto, “Patterns of New Physics in $b \rightarrow s\ell^+\ell^-$ transitions in the light of recent data,” JHEP **01** (2018), 093 doi:10.1007/JHEP01(2018)093 [arXiv:1704.05340 [hep-ph]].
- [54] M. Algueró, B. Capdevila, S. Descotes-Genon, P. Masjuan and J. Matias, “Are we overlooking lepton flavour universal new physics in $b \rightarrow s\ell\ell$?,” Phys. Rev. D **99** (2019) no.7, 075017 doi:10.1103/PhysRevD.99.075017 [arXiv:1809.08447 [hep-ph]].
- [55] J. Kumar and D. London, “New physics in $b \rightarrow se^+e^-$,” Phys. Rev. D **99**, no.7, 073008 (2019) doi:10.1103/PhysRevD.99.073008 [arXiv:1901.04516 [hep-ph]].
- [56] A. Datta, J. Kumar and D. London, “The B anomalies and new physics in $b \rightarrow se^+e^-$,” Phys. Lett. B **797** (2019), 134858 doi:10.1016/j.physletb.2019.134858 [arXiv:1903.10086 [hep-ph]].

- [57] B. Grzadkowski, M. Iskrzynski, M. Misiak and J. Rosiek, “dimension-6 Terms in the Standard Model Lagrangian,” JHEP **10**, 085 (2010) doi:10.1007/JHEP10(2010)085 [arXiv:1008.4884 [hep-ph]].
- [58] J. Aebischer, A. Crivellin, M. Fael and C. Greub, “Matching of gauge invariant dimension-6 operators for $b \rightarrow s$ and $b \rightarrow c$ transitions,” JHEP **05**, 037 (2016) doi:10.1007/JHEP05(2016)037 [arXiv:1512.02830 [hep-ph]].
- [59] A. Crivellin, C. Greub, D. Müller and F. Saturnino, “Importance of Loop Effects in Explaining the Accumulated Evidence for New Physics in B Decays with a Vector Leptoquark,” Phys. Rev. Lett. **122**, no.1, 011805 (2019) doi:10.1103/PhysRevLett.122.011805 [arXiv:1807.02068 [hep-ph]].
- [60] C. Bobeth and U. Haisch, “New Physics in Γ_{12}^s : $(\bar{s}b)(\bar{\tau}\tau)$ Operators,” Acta Phys. Polon. B **44** (2013), 127-176 doi:10.5506/APhysPolB.44.127 [arXiv:1109.1826 [hep-ph]].
- [61] J. Aebischer, W. Altmannshofer, D. Guadagnoli, M. Reboud, P. Stangl and D. M. Straub, “ B -decay discrepancies after Moriond 2019,” Eur. Phys. J. C **80**, no.3, 252 (2020) doi:10.1140/epjc/s10052-020-7817-x [arXiv:1903.10434 [hep-ph]].
- [62] J. E. Camargo-Molina, A. Celis and D. A. Faroughy, “Anomalies in Bottom from new physics in Top,” Phys. Lett. B **784**, 284-293 (2018) doi:10.1016/j.physletb.2018.07.051 [arXiv:1805.04917 [hep-ph]].
- [63] B. Capdevila, A. Crivellin, S. Descotes-Genon, L. Hofer and J. Matias, “Searching for New Physics with $b \rightarrow s\tau^+\tau^-$ processes,” Phys. Rev. Lett. **120** (2018) no.18, 181802 doi:10.1103/PhysRevLett.120.181802 [arXiv:1712.01919 [hep-ph]].
- [64] R. W. Brown, R. H. Hobbs, J. Smith and N. Stanko, “Intermediate boson. iii. virtual-boson effects in neutrino trident production,” Phys. Rev. D **6**, 3273-3292 (1972) doi:10.1103/PhysRevD.6.3273
- [65] A. J. Buras, J. Girrbach-Noe, C. Niehoff and D. M. Straub, “ $B \rightarrow K^{(*)}\nu\bar{\nu}$ decays in the Standard Model and beyond,” JHEP **02**, 184 (2015) doi:10.1007/JHEP02(2015)184 [arXiv:1409.4557 [hep-ph]].
- [66] J. Grygier *et al.* [Belle], “Search for $B \rightarrow h\nu\bar{\nu}$ decays with semileptonic tagging at Belle,” Phys. Rev. D **96**, no.9, 091101 (2017) doi:10.1103/PhysRevD.96.091101 [arXiv:1702.03224 [hep-ex]].
- [67] A. K. Alok, B. Bhattacharya, D. Kumar, J. Kumar, D. London and S. U. Sankar, “New physics in $b \rightarrow s\mu^+\mu^-$: Distinguishing models through CP-violating effects,” Phys. Rev. D **96**, no.1, 015034 (2017) doi:10.1103/PhysRevD.96.015034 [arXiv:1703.09247 [hep-ph]].

- [68] G. Aad *et al.* [ATLAS], “Search for high-mass dilepton resonances using 139 fb⁻¹ of pp collision data collected at $\sqrt{s}=13$ TeV with the ATLAS detector,” *Phys. Lett. B* **796**, 68-87 (2019) doi:10.1016/j.physletb.2019.07.016 [arXiv:1903.06248 [hep-ex]].
- [69] W. Altmannshofer, S. Gori, M. Pospelov and I. Yavin, “Quark flavor transitions in $L_\mu - L_\tau$ models,” *Phys. Rev. D* **89**, 095033 (2014) doi:10.1103/PhysRevD.89.095033 [arXiv:1403.1269 [hep-ph]].
- [70] A. Crivellin, G. D’Ambrosio and J. Heeck, “Explaining $h \rightarrow \mu^\pm \tau^\mp$, $B \rightarrow K^* \mu^+ \mu^-$ and $B \rightarrow K \mu^+ \mu^- / B \rightarrow K e^+ e^-$ in a two-Higgs-doublet model with gauged $L_\mu - L_\tau$,” *Phys. Rev. Lett.* **114**, 151801 (2015) doi:10.1103/PhysRevLett.114.151801 [arXiv:1501.00993 [hep-ph]].
- [71] A. Crivellin, G. D’Ambrosio and J. Heeck, “Addressing the LHC flavor anomalies with horizontal gauge symmetries,” *Phys. Rev. D* **91**, no.7, 075006 (2015) doi:10.1103/PhysRevD.91.075006 [arXiv:1503.03477 [hep-ph]].
- [72] W. Altmannshofer, S. Gori, S. Profumo and F. S. Queiroz, “Explaining dark matter and B decay anomalies with an $L_\mu - L_\tau$ model,” *JHEP* **12**, 106 (2016) doi:10.1007/JHEP12(2016)106 [arXiv:1609.04026 [hep-ph]].
- [73] A. Crivellin, J. Fuentes-Martin, A. Greljo and G. Isidori, “Lepton Flavor Non-Universality in B decays from Dynamical Yukawas,” *Phys. Lett. B* **766**, 77-85 (2017) doi:10.1016/j.physletb.2016.12.057 [arXiv:1611.02703 [hep-ph]].
- [74] P. Ko, T. Nomura and H. Okada, “Explaining $B \rightarrow K^{(*)} \ell^+ \ell^-$ anomaly by radiatively induced coupling in $U(1)_{\mu-\tau}$ gauge symmetry,” *Phys. Rev. D* **95**, no.11, 111701 (2017) doi:10.1103/PhysRevD.95.111701 [arXiv:1702.02699 [hep-ph]].
- [75] G. Arcadi, T. Hugle and F. S. Queiroz, “The Dark $L_\mu - L_\tau$ Rises via Kinetic Mixing,” *Phys. Lett. B* **784**, 151-158 (2018) doi:10.1016/j.physletb.2018.07.028 [arXiv:1803.05723 [hep-ph]].
- [76] S. Singirala, S. Sahoo and R. Mohanta, “Exploring dark matter, neutrino mass and $R_{K^{(*)},\phi}$ anomalies in $L_\mu - L_\tau$ model,” *Phys. Rev. D* **99**, no.3, 035042 (2019) doi:10.1103/PhysRevD.99.035042 [arXiv:1809.03213 [hep-ph]].
- [77] P. T. P. Hutaauruk, T. Nomura, H. Okada and Y. Orikasa, “Dark matter and B -meson anomalies in a flavor dependent gauge symmetry,” *Phys. Rev. D* **99**, no.5, 055041 (2019) doi:10.1103/PhysRevD.99.055041 [arXiv:1901.03932 [hep-ph]].
- [78] S. Baek, “Scalar dark matter behind $b \rightarrow s \mu \mu$ anomaly,” *JHEP* **05**, 104 (2019) doi:10.1007/JHEP05(2019)104 [arXiv:1901.04761 [hep-ph]].
- [79] A. Biswas and A. Shaw, “Reconciling dark matter, $R_{K^{(*)}}$ anomalies and $(g - 2)_\mu$ in an $L_\mu - L_\tau$ scenario,” *JHEP* **05**, 165 (2019) doi:10.1007/JHEP05(2019)165 [arXiv:1903.08745 [hep-ph]].

- [80] Z. L. Han, R. Ding, S. J. Lin and B. Zhu, “Gauged $U(1)_{L_\mu-L_\tau}$ scotogenic model in light of $R_{K^{(*)}}$ anomaly and AMS-02 positron excess,” *Eur. Phys. J. C* **79**, no.12, 1007 (2019) doi:10.1140/epjc/s10052-019-7526-5 [arXiv:1908.07192 [hep-ph]].
- [81] A. Crivellin, C. A. Manzari, M. Alguero and J. Matias, “Combined Explanation of the $Z \rightarrow b\bar{b}$ Forward-Backward Asymmetry, the Cabibbo Angle Anomaly, and $\tau \rightarrow \mu\nu\nu$ and $b \rightarrow s\ell + \ell^-$ Data,” *Phys. Rev. Lett.* **127**, no.1, 011801 (2021) doi:10.1103/PhysRevLett.127.011801 [arXiv:2010.14504 [hep-ph]].
- [82] P. Ko, T. Nomura and H. Okada, “A flavor dependent gauge symmetry, Predictive radiative seesaw and LHCb anomalies,” *Phys. Lett. B* **772**, 547-552 (2017) doi:10.1016/j.physletb.2017.07.021 [arXiv:1701.05788 [hep-ph]].
- [83] C. Bonilla, T. Modak, R. Srivastava and J. W. F. Valle, “ $U(1)_{B_3-3L_\mu}$ gauge symmetry as a simple description of $b \rightarrow s$ anomalies,” *Phys. Rev. D* **98**, no.9, 095002 (2018) doi:10.1103/PhysRevD.98.095002 [arXiv:1705.00915 [hep-ph]].
- [84] L. Bian, S. M. Choi, Y. J. Kang and H. M. Lee, “A minimal flavored $U(1)'$ for B -meson anomalies,” *Phys. Rev. D* **96**, no.7, 075038 (2017) doi:10.1103/PhysRevD.96.075038 [arXiv:1707.04811 [hep-ph]].
- [85] G. H. Duan, X. Fan, M. Frank, C. Han and J. M. Yang, “A minimal $U(1)'$ extension of MSSM in light of the B decay anomaly,” *Phys. Lett. B* **789**, 54-58 (2019) doi:10.1016/j.physletb.2018.12.005 [arXiv:1808.04116 [hep-ph]].
- [86] C. Q. Geng and H. Okada, “Resolving B -meson anomalies by flavor-dependent gauged symmetries $\prod_{i=1}^3 U(1)_{B_i-L_i}$,” [arXiv:1812.07918 [hep-ph]].
- [87] P. Ko, T. Nomura and C. Yu, “ $b \rightarrow s\mu^+\mu^-$ anomalies and related phenomenology in $U(1)_{B_3-x_\mu L_\mu-x_\tau L_\tau}$ flavor gauge models,” *JHEP* **04**, 102 (2019) doi:10.1007/JHEP04(2019)102 [arXiv:1902.06107 [hep-ph]].
- [88] B. C. Allanach, “ $U(1)_{B_3-L_2}$ explanation of the neutral current B -anomalies,” *Eur. Phys. J. C* **81**, no.1, 56 (2021) doi:10.1140/epjc/s10052-021-08855-w [arXiv:2009.02197 [hep-ph]].
- [89] J. Davighi, “Anomalous Z' bosons for anomalous B decays,” *JHEP* **08**, 101 (2021) doi:10.1007/JHEP08(2021)101 [arXiv:2105.06918 [hep-ph]].
- [90] Y. Chung, “Explaining the B anomalies in a Fundamental Composite Higgs Model with Gauged $U(1)_{SM_3-HB}$,” [arXiv:2110.03125 [hep-ph]].
- [91] R. Gauld, F. Goertz and U. Haisch, “An explicit Z' -boson explanation of the $B \rightarrow K^*\mu^+\mu^-$ anomaly,” *JHEP* **01**, 069 (2014) doi:10.1007/JHEP01(2014)069 [arXiv:1310.1082 [hep-ph]].

- [92] A. J. Buras, F. De Fazio and J. Girrbach, “331 models facing new $b \rightarrow s\mu^+\mu^-$ data,” JHEP **02**, 112 (2014) doi:10.1007/JHEP02(2014)112 [arXiv:1311.6729 [hep-ph]].
- [93] A. Celis, J. Fuentes-Martin, M. Jung and H. Serodio, “Family nonuniversal Z' models with protected flavor-changing interactions,” Phys. Rev. D **92**, no.1, 015007 (2015) doi:10.1103/PhysRevD.92.015007 [arXiv:1505.03079 [hep-ph]].
- [94] D. Aristizabal Sierra, F. Staub and A. Vicente, “Shedding light on the $b \rightarrow s$ anomalies with a dark sector,” Phys. Rev. D **92**, no.1, 015001 (2015) doi:10.1103/PhysRevD.92.015001 [arXiv:1503.06077 [hep-ph]].
- [95] G. Bélanger, C. Delaunay and S. Westhoff, “A Dark Matter Relic From Muon Anomalies,” Phys. Rev. D **92**, 055021 (2015) doi:10.1103/PhysRevD.92.055021 [arXiv:1507.06660 [hep-ph]].
- [96] A. Celis, W. Z. Feng and M. Vollmann, “Dirac dark matter and $b \rightarrow s\ell^+\ell^-$ with $U(1)$ gauge symmetry,” Phys. Rev. D **95**, no.3, 035018 (2017) doi:10.1103/PhysRevD.95.035018 [arXiv:1608.03894 [hep-ph]].
- [97] J. M. Cline, J. M. Cornell, D. London and R. Watanabe, “Hidden sector explanation of B -decay and cosmic ray anomalies,” Phys. Rev. D **95**, no.9, 095015 (2017) doi:10.1103/PhysRevD.95.095015 [arXiv:1702.00395 [hep-ph]].
- [98] R. Alonso, P. Cox, C. Han and T. T. Yanagida, “Flavoured $B - L$ local symmetry and anomalous rare B decays,” Phys. Lett. B **774**, 643-648 (2017) doi:10.1016/j.physletb.2017.10.027 [arXiv:1705.03858 [hep-ph]].
- [99] C. W. Chiang, X. G. He, J. Tandean and X. B. Yuan, “ $R_{K^{(*)}}$ and related $b \rightarrow s\ell\bar{\ell}$ anomalies in minimal flavor violation framework with Z' boson,” Phys. Rev. D **96**, no.11, 115022 (2017) doi:10.1103/PhysRevD.96.115022 [arXiv:1706.02696 [hep-ph]].
- [100] S. F. King, “Flavourful Z' models for $R_{K^{(*)}}$,” JHEP **08**, 019 (2017) doi:10.1007/JHEP08(2017)019 [arXiv:1706.06100 [hep-ph]].
- [101] J. M. Cline and J. Martin Camalich, “ B decay anomalies from non-abelian local horizontal symmetry,” Phys. Rev. D **96**, no.5, 055036 (2017) doi:10.1103/PhysRevD.96.055036 [arXiv:1706.08510 [hep-ph]].
- [102] A. Falkowski, S. F. King, E. Perdomo and M. Pierre, “Flavourful Z' portal for vector-like neutrino Dark Matter and $R_{K^{(*)}}$,” JHEP **08**, 061 (2018) doi:10.1007/JHEP08(2018)061 [arXiv:1803.04430 [hep-ph]].
- [103] S. Baek and C. Yu, “Dark matter for $b \rightarrow s\mu^+\mu^-$ anomaly in a gauged $U(1)_X$ model,” JHEP **11**, 054 (2018) doi:10.1007/JHEP11(2018)054 [arXiv:1806.05967 [hep-ph]].
- [104] B. C. Allanach and J. Davighi, “Third family hypercharge model for $R_{K^{(*)}}$ and aspects of the fermion mass problem,” JHEP **12**, 075 (2018) doi:10.1007/JHEP12(2018)075 [arXiv:1809.01158 [hep-ph]].

- [105] B. Capdevila, A. Crivellin, C. A. Manzari and M. Montull, “Explaining $b \rightarrow s\ell^+\ell^-$ and the Cabibbo Angle Anomaly with a Vector Triplet,” *Phys. Rev. D* **103**, 015032 (2021) doi:10.1103/PhysRevD.103.015032 [arXiv:2005.13542 [hep-ph]].
- [106] A. J. Buras and J. Girrbach, “Left-handed Z' and Z FCNC quark couplings facing new $b \rightarrow s\mu^+\mu^-$ data,” *JHEP* **12**, 009 (2013) doi:10.1007/JHEP12(2013)009 [arXiv:1309.2466 [hep-ph]].
- [107] A. Falkowski, M. Nardecchia and R. Ziegler, “Lepton Flavor Non-Universality in B -meson Decays from a $U(2)$ Flavor Model,” *JHEP* **11**, 173 (2015) doi:10.1007/JHEP11(2015)173 [arXiv:1509.01249 [hep-ph]].
- [108] A. Celis, W. Z. Feng and D. Lüst, “Stringy explanation of $bt\ell^+\ell^-$ anomalies,” *JHEP* **02**, 007 (2016) doi:10.1007/JHEP02(2016)007 [arXiv:1512.02218 [hep-ph]].
- [109] C. W. Chiang, X. G. He and G. Valencia, “ Z' model for $b \rightarrow s\ell\ell$ flavor anomalies,” *Phys. Rev. D* **93**, no.7, 074003 (2016) doi:10.1103/PhysRevD.93.074003 [arXiv:1601.07328 [hep-ph]].
- [110] P. Ko, Y. Omura, Y. Shigekami and C. Yu, “LHCb anomaly and B physics in flavored Z' models with flavored Higgs doublets,” *Phys. Rev. D* **95**, no.11, 115040 (2017) doi:10.1103/PhysRevD.95.115040 [arXiv:1702.08666 [hep-ph]].
- [111] B. C. Allanach and J. Davighi, “Naturalising the third family hypercharge model for neutral current B -anomalies,” *Eur. Phys. J. C* **79**, no.11, 908 (2019) doi:10.1140/epjc/s10052-019-7414-z [arXiv:1905.10327 [hep-ph]].
- [112] W. Altmannshofer, J. Davighi and M. Nardecchia, “Gauging the accidental symmetries of the standard model, and implications for the flavor anomalies,” *Phys. Rev. D* **101**, no.1, 015004 (2020) doi:10.1103/PhysRevD.101.015004 [arXiv:1909.02021 [hep-ph]].
- [113] F. Sala and D. M. Straub, “A New Light Particle in B Decays?,” *Phys. Lett. B* **774**, 205-209 (2017) doi:10.1016/j.physletb.2017.09.072 [arXiv:1704.06188 [hep-ph]].
- [114] F. Bishara, U. Haisch and P. F. Monni, “Regarding light resonance interpretations of the B decay anomalies,” *Phys. Rev. D* **96**, no.5, 055002 (2017) doi:10.1103/PhysRevD.96.055002 [arXiv:1705.03465 [hep-ph]].
- [115] L. Darmé, M. Fedele, K. Kowalska and E. M. Sessolo, “Flavour anomalies from a split dark sector,” *JHEP* **08**, 148 (2020) doi:10.1007/JHEP08(2020)148 [arXiv:2002.11150 [hep-ph]].
- [116] L. Darmé, M. Fedele, K. Kowalska and E. M. Sessolo, “Flavour anomalies and the muon $g - 2$ from feebly interacting particles,” [arXiv:2106.12582 [hep-ph]].

- [117] R. Alonso, B. Grinstein and J. Martin Camalich, “Lepton universality violation and lepton flavor conservation in B -meson decays,” JHEP **10**, 184 (2015) doi:10.1007/JHEP10(2015)184 [arXiv:1505.05164 [hep-ph]].
- [118] Y. Sakaki, M. Tanaka, A. Tayduganov and R. Watanabe, “Testing leptoquark models in $\bar{B} \rightarrow D^{(*)}\tau\bar{\nu}$,” Phys. Rev. D **88**, no.9, 094012 (2013) doi:10.1103/PhysRevD.88.094012 [arXiv:1309.0301 [hep-ph]].
- [119] G. Hiller and M. Schmaltz, “ R_K and future $b \rightarrow sll$ physics beyond the standard model opportunities,” Phys. Rev. D **90**, 054014 (2014) doi:10.1103/PhysRevD.90.054014 [arXiv:1408.1627 [hep-ph]].
- [120] B. Gripaios, M. Nardecchia and S. A. Renner, “Composite leptoquarks and anomalies in B -meson decays,” JHEP **05**, 006 (2015) doi:10.1007/JHEP05(2015)006 [arXiv:1412.1791 [hep-ph]].
- [121] I. de Medeiros Varzielas and G. Hiller, “Clues for flavor from rare lepton and quark decays,” JHEP **06**, 072 (2015) doi:10.1007/JHEP06(2015)072 [arXiv:1503.01084 [hep-ph]].
- [122] S. Sahoo and R. Mohanta, “Scalar leptoquarks and the rare B meson decays,” Phys. Rev. D **91**, no.9, 094019 (2015) doi:10.1103/PhysRevD.91.094019 [arXiv:1501.05193 [hep-ph]].
- [123] G. Hiller and I. Nisandzic, “ R_K and R_{K^*} beyond the standard model,” Phys. Rev. D **96**, no.3, 035003 (2017) doi:10.1103/PhysRevD.96.035003 [arXiv:1704.05444 [hep-ph]].
- [124] J. M. Cline, “ B decay anomalies and dark matter from vectorlike confinement,” Phys. Rev. D **97**, no.1, 015013 (2018) doi:10.1103/PhysRevD.97.015013 [arXiv:1710.02140 [hep-ph]].
- [125] D. Bečirević, N. Košnik, O. Sumensari and R. Zukanovich Funchal, “Palatable Leptoquark Scenarios for Lepton Flavor Violation in Exclusive $b \rightarrow s\ell_1\ell_2$ modes,” JHEP **11**, 035 (2016) doi:10.1007/JHEP11(2016)035 [arXiv:1608.07583 [hep-ph]].
- [126] A. K. Alok, S. Kumbhakar and S. Uma Sankar, “A unique discrimination between new physics scenarios in $b \rightarrow s\mu^+\mu^-$ anomalies,” [arXiv:2001.04395 [hep-ph]].
- [127] Y. Amhis et al. (HFLAV), Eur. Phys. J. **C77**, 895 (2017), “Updated average of $R(D)$ and $R(D^*)$ for Spring 2019” at <https://hflav-eos.web.cern.ch/hflav-eos/semi/spring19/html/RDsDsstar/RDRDs.html>.
- [128] R. Watanabe, “New Physics effect on $B_c \rightarrow J/\psi\tau\bar{\nu}$ in relation to the $R_{D^{(*)}}$ anomaly,” Phys. Lett. B **776**, 5-9 (2018) doi:10.1016/j.physletb.2017.11.016 [arXiv:1709.08644 [hep-ph]].

- [129] S. Hirose *et al.* [Belle], “Measurement of the τ lepton polarization and $R(D^*)$ in the decay $\bar{B} \rightarrow D^* \tau^- \bar{\nu}_\tau$,” *Phys. Rev. Lett.* **118**, no.21, 211801 (2017) doi:10.1103/PhysRevLett.118.211801 [arXiv:1612.00529 [hep-ex]].
- [130] S. Hirose *et al.* [Belle], “Measurement of the τ lepton polarization and $R(D^*)$ in the decay $\bar{B} \rightarrow D^* \tau^- \bar{\nu}_\tau$ with one-prong hadronic τ decays at Belle,” *Phys. Rev. D* **97**, no.1, 012004 (2018) doi:10.1103/PhysRevD.97.012004 [arXiv:1709.00129 [hep-ex]].
- [131] K. Adamczyk, “B to semitauonic decays at Belle/Belle II,” (2018), talk at 10th International Workshop on the CKM Unitarity Triangle, Heidelberg, 17-21 Sep 2018.
- [132] M. Algueró, S. Descotes-Genon, J. Matias and M. Novoa-Brunet, “Symmetries in $B \rightarrow D^* \ell \nu$ angular observables,” *JHEP* **06** (2020), 156 doi:10.1007/JHEP06(2020)156 [arXiv:2003.02533 [hep-ph]].
- [133] R. Alonso, B. Grinstein and J. Martin Camalich, “Lifetime of B_c^- Constrains Explanations for Anomalies in $B \rightarrow D^{(*)} \tau \nu$,” *Phys. Rev. Lett.* **118**, no.8, 081802 (2017) doi:10.1103/PhysRevLett.118.081802 [arXiv:1611.06676 [hep-ph]].
- [134] A. G. Akeroyd and C. H. Chen, “Constraint on the branching ratio of $B_c \rightarrow \tau \bar{\nu}$ from LEP1 and consequences for $R(D^{(*)})$ anomaly,” *Phys. Rev. D* **96**, no.7, 075011 (2017) doi:10.1103/PhysRevD.96.075011 [arXiv:1708.04072 [hep-ph]].
- [135] M. Blanke, A. Crivellin, S. de Boer, T. Kitahara, M. Moscati, U. Nierste and I. Nišandžić, “Impact of polarization observables and $B_c \rightarrow \tau \nu$ on new physics explanations of the $b \rightarrow c \tau \nu$ anomaly,” *Phys. Rev. D* **99**, no.7, 075006 (2019) doi:10.1103/PhysRevD.99.075006 [arXiv:1811.09603 [hep-ph]].
- [136] M. Jung and D. M. Straub, “Constraining new physics in $b \rightarrow c \ell \nu$ transitions,” *JHEP* **01**, 009 (2019) doi:10.1007/JHEP01(2019)009 [arXiv:1801.01112 [hep-ph]].
- [137] C.P. Burgess, S. Hamoudou, J. Kumar and D. London, “Beyond SMEFT with $b \rightarrow c \tau^- \bar{\nu}$,” [arXiv:2111.07421 [hep-ph]]
- [138] O. Catà and M. Jung, “Signatures of a nonstandard Higgs boson from flavor physics,” *Phys. Rev. D* **92**, no.5, 055018 (2015) doi:10.1103/PhysRevD.92.055018 [arXiv:1505.05804 [hep-ph]].
- [139] M. Blanke, A. Crivellin, T. Kitahara, M. Moscati, U. Nierste and I. Nišandžić, “Addendum to “Impact of polarization observables and $B_c \rightarrow \tau \nu$ on new physics explanations of the $b \rightarrow c \tau \nu$ anomaly”,” doi:10.1103/PhysRevD.100.035035 [arXiv:1905.08253 [hep-ph]].
- [140] D. Bečirević, S. Fajfer, N. Košnik and O. Sumensari, “Leptoquark model to explain the B -physics anomalies, R_K and R_D ,” *Phys. Rev. D* **94**, no.11, 115021 (2016) doi:10.1103/PhysRevD.94.115021 [arXiv:1608.08501 [hep-ph]].

- [141] D. Bečirević, I. Doršner, S. Fajfer, N. Košnik, D. A. Faroughy and O. Sumensari, “Scalar leptoquarks from grand unified theories to accommodate the B -physics anomalies,” *Phys. Rev. D* **98**, no.5, 055003 (2018) doi:10.1103/PhysRevD.98.055003 [arXiv:1806.05689 [hep-ph]].
- [142] S. Fajfer, J. F. Kamenik, I. Nisandzic and J. Zupan, “Implications of Lepton Flavor Universality Violations in B Decays,” *Phys. Rev. Lett.* **109**, 161801 (2012) doi:10.1103/PhysRevLett.109.161801 [arXiv:1206.1872 [hep-ph]].
- [143] M. Tanaka and R. Watanabe, “New physics in the weak interaction of $\bar{B} \rightarrow D^{(*)}\tau\bar{\nu}$,” *Phys. Rev. D* **87**, no.3, 034028 (2013) doi:10.1103/PhysRevD.87.034028 [arXiv:1212.1878 [hep-ph]].
- [144] M. Freytsis, Z. Ligeti and J. T. Ruderman, “Flavor models for $\bar{B} \rightarrow D^{(*)}\tau\bar{\nu}$,” *Phys. Rev. D* **92**, no.5, 054018 (2015) doi:10.1103/PhysRevD.92.054018 [arXiv:1506.08896 [hep-ph]].
- [145] A. K. Alok, D. Kumar, J. Kumar, S. Kumbhakar and S. U. Sankar, “New physics solutions for R_D and R_{D^*} ,” *JHEP* **09**, 152 (2018) doi:10.1007/JHEP09(2018)152 [arXiv:1710.04127 [hep-ph]].
- [146] P. Asadi, M. R. Buckley and D. Shih, “It’s all right(-handed neutrinos): a new W' model for the $R_{D^{(*)}}$ anomaly,” *JHEP* **09**, 010 (2018) doi:10.1007/JHEP09(2018)010 [arXiv:1804.04135 [hep-ph]].
- [147] A. Greljo, D. J. Robinson, B. Shakya and J. Zupan, “ $R(D^{(*)})$ from W' and right-handed neutrinos,” *JHEP* **09**, 169 (2018) doi:10.1007/JHEP09(2018)169 [arXiv:1804.04642 [hep-ph]].
- [148] D. J. Robinson, B. Shakya and J. Zupan, “Right-handed neutrinos and $R(D^{(*)})$,” *JHEP* **02**, 119 (2019) doi:10.1007/JHEP02(2019)119 [arXiv:1807.04753 [hep-ph]].
- [149] K. S. Babu, B. Dutta and R. N. Mohapatra, “A theory of $R(D^*, D)$ anomaly with right-handed currents,” *JHEP* **01**, 168 (2019) doi:10.1007/JHEP01(2019)168 [arXiv:1811.04496 [hep-ph]].
- [150] R. Mandal, C. Murgui, A. Peñuelas and A. Pich, “The role of right-handed neutrinos in $b \rightarrow c\tau\bar{\nu}$ anomalies,” *JHEP* **08**, no.08, 022 (2020) doi:10.1007/JHEP08(2020)022 [arXiv:2004.06726 [hep-ph]].
- [151] J. D. Gómez, N. Quintero and E. Rojas, “Charged current $b \rightarrow c\tau\bar{\nu}_\tau$ anomalies in a general W' boson scenario,” *Phys. Rev. D* **100**, no.9, 093003 (2019) doi:10.1103/PhysRevD.100.093003 [arXiv:1907.08357 [hep-ph]].
- [152] X. Q. Li, Y. D. Yang and X. Zhang, “Revisiting the one leptoquark solution to the $R(D^{(*)})$ anomalies and its phenomenological implications,” *JHEP* **08**, 054 (2016) doi:10.1007/JHEP08(2016)054 [arXiv:1605.09308 [hep-ph]].

- [153] S. Bansal, R. M. Capdevilla and C. Kolda, “Constraining the minimal flavor violating leptoquark explanation of the $R_{D^{(*)}}$ anomaly,” Phys. Rev. D **99**, no.3, 035047 (2019) doi:10.1103/PhysRevD.99.035047 [arXiv:1810.11588 [hep-ph]].
- [154] U. Aydemir, T. Mandal and S. Mitra, “Addressing the $\mathbf{R}_{D^{(*)}}$ anomalies with an \mathbf{S}_1 leptoquark from $\mathbf{SO}(10)$ grand unification,” Phys. Rev. D **101**, no.1, 015011 (2020) doi:10.1103/PhysRevD.101.015011 [arXiv:1902.08108 [hep-ph]].
- [155] K. Cheung, Z. R. Huang, H. D. Li, C. D. Lü, Y. N. Mao and R. Y. Tang, “Revisit to the $b \rightarrow c\tau\nu$ transition: In and beyond the SM,” Nucl. Phys. B **965**, 115354 (2021) doi:10.1016/j.nuclphysb.2021.115354 [arXiv:2002.07272 [hep-ph]].
- [156] A. Crivellin, C. Greub and A. Kokulu, “Explaining $B \rightarrow D\tau\nu$, $B \rightarrow D^*\tau\nu$ and $B \rightarrow \tau\nu$ in a 2HDM of type III,” Phys. Rev. D **86**, 054014 (2012) doi:10.1103/PhysRevD.86.054014 [arXiv:1206.2634 [hep-ph]].
- [157] A. Celis, M. Jung, X. Q. Li and A. Pich, “Sensitivity to charged scalars in $B \rightarrow D^{(*)}\tau\nu_\tau$ and $B \rightarrow \tau\nu_\tau$ decays,” JHEP **01**, 054 (2013) doi:10.1007/JHEP01(2013)054 [arXiv:1210.8443 [hep-ph]].
- [158] A. Crivellin, J. Heeck and P. Stoffer, “A perturbed lepton-specific two-Higgs-doublet model facing experimental hints for physics beyond the Standard Model,” Phys. Rev. Lett. **116**, no.8, 081801 (2016) doi:10.1103/PhysRevLett.116.081801 [arXiv:1507.07567 [hep-ph]].
- [159] M. Wei and Y. Chong-Xing, “Charged Higgs bosons from the 3-3-1 models and the $\mathcal{R}(D^{(*)})$ anomalies,” Phys. Rev. D **95**, no.3, 035040 (2017) doi:10.1103/PhysRevD.95.035040 [arXiv:1702.01255 [hep-ph]].
- [160] C. H. Chen and T. Nomura, “Charged-Higgs on $R_{D^{(*)}}$, τ polarization, and FBA,” Eur. Phys. J. C **77**, no.9, 631 (2017) doi:10.1140/epjc/s10052-017-5198-6 [arXiv:1703.03646 [hep-ph]].
- [161] J. P. Lee, “ $B \rightarrow D^{(*)}\tau\nu_\tau$ in the 2HDM with an anomalous τ coupling,” Phys. Rev. D **96**, no.5, 055005 (2017) doi:10.1103/PhysRevD.96.055005 [arXiv:1705.02465 [hep-ph]].
- [162] S. Iguro and K. Tobe, “ $R(D^{(*)})$ in a general two Higgs doublet model,” Nucl. Phys. B **925**, 560-606 (2017) doi:10.1016/j.nuclphysb.2017.10.014 [arXiv:1708.06176 [hep-ph]].
- [163] R. Martinez, C. F. Sierra and G. Valencia, “Beyond $\mathcal{R}(D^{(*)})$ with the general type-III 2HDM for $b \rightarrow c\tau\nu$,” Phys. Rev. D **98**, no.11, 115012 (2018) doi:10.1103/PhysRevD.98.115012 [arXiv:1805.04098 [hep-ph]].
- [164] S. Fraser, C. Marzo, L. Marzola, M. Raidal and C. Spethmann, “Towards a viable scalar interpretation of $R_{D^{(*)}}$,” Phys. Rev. D **98**, no.3, 035016 (2018) doi:10.1103/PhysRevD.98.035016 [arXiv:1805.08189 [hep-ph]].

- [165] J. Cardozo, J. H. Muñoz, N. Quintero and E. Rojas, “Analysing the charged scalar boson contribution to the charged-current B meson anomalies,” *J. Phys. G* **48**, no.3, 035001 (2021) doi:10.1088/1361-6471/abc865 [arXiv:2006.07751 [hep-ph]].
- [166] S. Iguro, Y. Omura and M. Takeuchi, “Test of the $R(D^{(*)})$ anomaly at the LHC,” *Phys. Rev. D* **99**, no.7, 075013 (2019) doi:10.1103/PhysRevD.99.075013 [arXiv:1810.05843 [hep-ph]].
- [167] Y. Sakaki, M. Tanaka, A. Tayduganov and R. Watanabe, “Probing New Physics with q^2 distributions in $\bar{B} \rightarrow D^{(*)}\tau\bar{\nu}$,” *Phys. Rev. D* **91**, no.11, 114028 (2015) doi:10.1103/PhysRevD.91.114028 [arXiv:1412.3761 [hep-ph]].
- [168] A. K. Alok, D. Kumar, S. Kumbhakar and S. U. Sankar, “ D^* polarization as a probe to discriminate new physics in $\bar{B} \rightarrow D^*\tau\bar{\nu}$,” *Phys. Rev. D* **95**, no.11, 115038 (2017) doi:10.1103/PhysRevD.95.115038 [arXiv:1606.03164 [hep-ph]].
- [169] S. Iguro, T. Kitahara, Y. Omura, R. Watanabe and K. Yamamoto, “ D^* polarization vs. $R_{D^{(*)}}$ anomalies in the leptoquark models,” *JHEP* **02**, 194 (2019) doi:10.1007/JHEP02(2019)194 [arXiv:1811.08899 [hep-ph]].
- [170] M. A. Ivanov, J. G. Körner and C. T. Tran, “Probing new physics in $\bar{B}^0 \rightarrow D^{(*)}\tau^-\bar{\nu}_\tau$ using the longitudinal, transverse, and normal polarization components of the tau lepton,” *Phys. Rev. D* **95**, no.3, 036021 (2017) doi:10.1103/PhysRevD.95.036021 [arXiv:1701.02937 [hep-ph]].
- [171] B. Bhattacharya, A. Datta, S. Kamali and D. London, “A measurable angular distribution for $\bar{B} \rightarrow D^*\tau^-\bar{\nu}_\tau$ decays,” *JHEP* **07**, no.07, 194 (2020) doi:10.1007/JHEP07(2020)194 [arXiv:2005.03032 [hep-ph]].
- [172] B. Bhattacharya, A. Datta, D. London and S. Shivashankara, “Simultaneous Explanation of the R_K and $R(D^{(*)})$ Puzzles,” *Phys. Lett. B* **742**, 370-374 (2015) doi:10.1016/j.physletb.2015.02.011 [arXiv:1412.7164 [hep-ph]].
- [173] A. Greljo, G. Isidori and D. Marzocca, “On the breaking of Lepton Flavor Universality in B decays,” *JHEP* **07**, 142 (2015) doi:10.1007/JHEP07(2015)142 [arXiv:1506.01705 [hep-ph]].
- [174] L. Calibbi, A. Crivellin and T. Ota, “Effective Field Theory Approach to $b \rightarrow s\ell\ell'$, $B \rightarrow K^{(*)}\nu\bar{\nu}$ and $B \rightarrow D^{(*)}\tau\nu$ with Third Generation Couplings,” *Phys. Rev. Lett.* **115**, 181801 (2015) doi:10.1103/PhysRevLett.115.181801 [arXiv:1506.02661 [hep-ph]].
- [175] J. Kumar, D. London and R. Watanabe, “Combined Explanations of the $b \rightarrow s\mu^+\mu^-$ and $b \rightarrow c\tau^-\bar{\nu}$ Anomalies: a General Model Analysis,” *Phys. Rev. D* **99**, no.1, 015007 (2019) doi:10.1103/PhysRevD.99.015007 [arXiv:1806.07403 [hep-ph]].

- [176] S. M. Boucenna, A. Celis, J. Fuentes-Martin, A. Vicente and J. Virto, “Phenomenology of an $SU(2) \times SU(2) \times U(1)$ model with lepton-flavour non-universality,” JHEP **12**, 059 (2016) doi:10.1007/JHEP12(2016)059 [arXiv:1608.01349 [hep-ph]].
- [177] B. Bhattacharya, A. Datta, J. P. Guévin, D. London and R. Watanabe, “Simultaneous Explanation of the R_K and $R_{D^{(*)}}$ Puzzles: a Model Analysis,” JHEP **01**, 015 (2017) doi:10.1007/JHEP01(2017)015 [arXiv:1609.09078 [hep-ph]].
- [178] D. Buttazzo, A. Greljo, G. Isidori and D. Marzocca, “B-physics anomalies: a guide to combined explanations,” JHEP **11**, 044 (2017) doi:10.1007/JHEP11(2017)044 [arXiv:1706.07808 [hep-ph]].
- [179] R. Barbieri, G. Isidori, A. Pattori and F. Senia, “Anomalies in B -decays and $U(2)$ flavour symmetry,” Eur. Phys. J. C **76**, no.2, 67 (2016) doi:10.1140/epjc/s10052-016-3905-3 [arXiv:1512.01560 [hep-ph]].
- [180] A. Angelescu, D. Bečirević, D. A. Faroughy, F. Jaffredo and O. Sumensari, “Single leptoquark solutions to the B-physics anomalies,” Phys. Rev. D **104**, no.5, 055017 (2021) doi:10.1103/PhysRevD.104.055017 [arXiv:2103.12504 [hep-ph]].
- [181] A. Crivellin, D. Müller and T. Ota, “Simultaneous explanation of $R(D^{(*)})$ and $b \rightarrow s\mu^+\mu^-$: the last scalar leptoquarks standing,” JHEP **09**, 040 (2017) doi:10.1007/JHEP09(2017)040 [arXiv:1703.09226 [hep-ph]].
- [182] N. Assad, B. Fornal and B. Grinstein, “Baryon Number and Lepton Universality Violation in Leptoquark and Diquark Models,” Phys. Lett. B **777**, 324-331 (2018) doi:10.1016/j.physletb.2017.12.042 [arXiv:1708.06350 [hep-ph]].
- [183] L. Di Luzio, A. Greljo and M. Nardecchia, “Gauge leptoquark as the origin of B -physics anomalies,” Phys. Rev. D **96**, no.11, 115011 (2017) doi:10.1103/PhysRevD.96.115011 [arXiv:1708.08450 [hep-ph]].
- [184] L. Calibbi, A. Crivellin and T. Li, “Model of vector leptoquarks in view of the B -physics anomalies,” Phys. Rev. D **98**, no.11, 115002 (2018) doi:10.1103/PhysRevD.98.115002 [arXiv:1709.00692 [hep-ph]].
- [185] M. Bordone, C. Cornella, J. Fuentes-Martin and G. Isidori, “A three-site gauge model for flavor hierarchies and flavor anomalies,” Phys. Lett. B **779**, 317-323 (2018) doi:10.1016/j.physletb.2018.02.011 [arXiv:1712.01368 [hep-ph]].
- [186] R. Barbieri and A. Tesi, “ B -decay anomalies in Pati-Salam $SU(4)$,” Eur. Phys. J. C **78**, no.3, 193 (2018) doi:10.1140/epjc/s10052-018-5680-9 [arXiv:1712.06844 [hep-ph]].
- [187] M. Blanke and A. Crivellin, “ B Meson Anomalies in a Pati-Salam Model within the Randall-Sundrum Background,” Phys. Rev. Lett. **121**, no.1, 011801 (2018) doi:10.1103/PhysRevLett.121.011801 [arXiv:1801.07256 [hep-ph]].

- [188] U. Aydemir, D. Minic, C. Sun and T. Takeuchi, “ B -decay anomalies and scalar leptoquarks in unified Pati-Salam models from noncommutative geometry,” *JHEP* **09**, 117 (2018) doi:10.1007/JHEP09(2018)117 [arXiv:1804.05844 [hep-ph]].
- [189] J. Heeck and D. Teresi, “Pati-Salam explanations of the B -meson anomalies,” *JHEP* **12**, 103 (2018) doi:10.1007/JHEP12(2018)103 [arXiv:1808.07492 [hep-ph]].
- [190] S. Balaji, R. Foot and M. A. Schmidt, “Chiral $SU(4)$ explanation of the $b \rightarrow s$ anomalies,” *Phys. Rev. D* **99**, no.1, 015029 (2019) doi:10.1103/PhysRevD.99.015029 [arXiv:1809.07562 [hep-ph]].
- [191] B. Fornal, S. A. Gadam and B. Grinstein, “Left-Right $SU(4)$ Vector Leptoquark Model for Flavor Anomalies,” *Phys. Rev. D* **99**, no.5, 055025 (2019) doi:10.1103/PhysRevD.99.055025 [arXiv:1812.01603 [hep-ph]].
- [192] S. Balaji and M. A. Schmidt, “Unified $SU(4)$ theory for the $R_{D^{(*)}}$ and $R_{K^{(*)}}$ anomalies,” *Phys. Rev. D* **101**, no.1, 015026 (2020) doi:10.1103/PhysRevD.101.015026 [arXiv:1911.08873 [hep-ph]].
- [193] S. Iguro, J. Kawamura, S. Okawa and Y. Omura, “TeV-scale vector leptoquark from Pati-Salam unification with vectorlike families,” *Phys. Rev. D* **104**, no.7, 075008 (2021) doi:10.1103/PhysRevD.104.075008 [arXiv:2103.11889 [hep-ph]].
- [194] A. Greljo and B. A. Stefanek, “Third family quark-lepton unification at the TeV scale,” *Phys. Lett. B* **782**, 131-138 (2018) doi:10.1016/j.physletb.2018.05.033 [arXiv:1802.04274 [hep-ph]].
- [195] C. Cornella, J. Fuentes-Martin and G. Isidori, “Revisiting the vector leptoquark explanation of the B -physics anomalies,” *JHEP* **1907**, 168 (2019) doi:10.1007/JHEP07(2019)168 [arXiv:1903.11517 [hep-ph]].
- [196] D. Guadagnoli, M. Reboud and P. Stangl, “The Dark Side of 4321,” *JHEP* **10**, 084 (2020) doi:10.1007/JHEP10(2020)084 [arXiv:2005.10117 [hep-ph]].
- [197] A. Crivellin, C. A. Manzari, M. Alguero and J. Matias, “Combined Explanation of the $Z \rightarrow b\bar{b}$ Forward-Backward Asymmetry, the Cabibbo Angle Anomaly, and $\tau \rightarrow \mu\nu\nu$ and $b \rightarrow s\ell + \ell$ Data,” *Phys. Rev. Lett.* **127** (2021) no.1, 011801 doi:10.1103/PhysRevLett.127.011801 [arXiv:2010.14504 [hep-ph]].
- [198] A. Vicente, “Flavor and Dark Matter connection,” *Springer Proc. Phys.* **234**, 393-400 (2019) doi:10.1007/978-3-030-29622-3_54 [arXiv:1812.03028 [hep-ph]].
- [199] D. Borah, L. Mukherjee and S. Nandi, “Low scale $U(1)_X$ gauge symmetry as an origin of dark matter, neutrino mass and flavour anomalies,” *JHEP* **12**, 052 (2020) doi:10.1007/JHEP12(2020)052 [arXiv:2007.13778 [hep-ph]].
- [200] S. M. Choi, Y. J. Kang, H. M. Lee and T. G. Ro, “Lepto-Quark Portal Dark Matter,” *JHEP* **10**, 104 (2018) doi:10.1007/JHEP10(2018)104 [arXiv:1807.06547 [hep-ph]].

- [201] M. J. Baker, D. A. Faroughy and S. Trifinopoulos, “Collider Signatures of Coannihilating Dark Matter in Light of the B-Physics Anomalies,” [arXiv:2109.08689 [hep-ph]].
- [202] B. Abi *et al.* [Muon $g-2$], “Measurement of the Positive Muon Anomalous Magnetic Moment to 0.46 ppm,” Phys. Rev. Lett. **126**, no.14, 141801 (2021) doi:10.1103/PhysRevLett.126.141801 [arXiv:2104.03281 [hep-ex]].
- [203] A. Greljo, P. Stangl and A. E. Thomsen, “A model of muon anomalies,” Phys. Lett. B **820**, 136554 (2021) doi:10.1016/j.physletb.2021.136554 [arXiv:2103.13991 [hep-ph]].
- [204] M. F. Navarro and S. F. King, “Fermiophobic Z' model for simultaneously explaining the muon anomalies $R_{K^{(*)}}$ and $(g-2)_\mu$,” [arXiv:2109.08729 [hep-ph]].
- [205] X. Wang, “Muon $(g-2)$ and Flavor Puzzles in the $U(1)_X$ -gauged Leptoquark Model,” [arXiv:2108.01279 [hep-ph]].
- [206] A. Greljo, Y. Soreq, P. Stangl, A. E. Thomsen and J. Zupan, “Muonic Force Behind Flavor Anomalies,” [arXiv:2107.07518 [hep-ph]].
- [207] P. F. Perez, C. Murgui and A. D. Plascencia, “Leptoquarks and matter unification: Flavor anomalies and the muon $g-2$,” Phys. Rev. D **104**, no.3, 035041 (2021) doi:10.1103/PhysRevD.104.035041 [arXiv:2104.11229 [hep-ph]].
- [208] K. Ban, Y. Jho, Y. Kwon, S. C. Park, S. Park and P. Y. Tseng, “A comprehensive study of vector leptoquark on the B -meson and Muon $g-2$ anomalies,” [arXiv:2104.06656 [hep-ph]].
- [209] M. Du, J. Liang, Z. Liu and V. Tran, “A vector leptoquark interpretation of the muon $g-2$ and B anomalies,” [arXiv:2104.05685 [hep-ph]].
- [210] D. Marzocca and S. Trifinopoulos, “Minimal Explanation of Flavor Anomalies: B-Meson Decays, Muon Magnetic Moment, and the Cabibbo Angle,” Phys. Rev. Lett. **127**, no.6, 2021 (2021) doi:10.1103/PhysRevLett.127.061803 [arXiv:2104.05730 [hep-ph]].
- [211] J. Y. Cen, Y. Cheng, X. G. He and J. Sun, “Flavor Specific $U(1)_{B_q-L_\mu}$ Gauge Model for Muon $g-2$ and $b \rightarrow s\bar{\mu}\mu$ Anomalies,” [arXiv:2104.05006 [hep-ph]].
- [212] I. Bigaran, J. Gargalionis and R. R. Volkas, “A near-minimal leptoquark model for reconciling flavour anomalies and generating radiative neutrino masses,” JHEP **10**, 106 (2019) doi:10.1007/JHEP10(2019)106 [arXiv:1906.01870 [hep-ph]].
- [213] P. S. Bhupal Dev, R. Mohanta, S. Patra and S. Sahoo, “Unified explanation of flavor anomalies, radiative neutrino masses, and ANITA anomalous events in a vector leptoquark model,” Phys. Rev. D **102**, no.9, 095012 (2020) doi:10.1103/PhysRevD.102.095012 [arXiv:2004.09464 [hep-ph]].

- [214] S. Saad, “Combined explanations of $(g - 2)_\mu$, $R_{D^{(*)}}$, $R_{K^{(*)}}$ anomalies in a two-loop radiative neutrino mass model,” *Phys. Rev. D* **102**, no.1, 015019 (2020) doi:10.1103/PhysRevD.102.015019 [arXiv:2005.04352 [hep-ph]].
- [215] K. S. Babu, P. S. B. Dev, S. Jana and A. Thapa, “Unified framework for B -anomalies, muon $g-2$ and neutrino masses,” *JHEP* **03**, 179 (2021) doi:10.1007/JHEP03(2021)179 [arXiv:2009.01771 [hep-ph]].
- [216] N. B. Beaudry, A. Datta, D. London, A. Rashed and J. S. Roux, “The $B \rightarrow \pi K$ puzzle revisited,” *JHEP* **01**, 074 (2018) doi:10.1007/JHEP01(2018)074 [arXiv:1709.07142 [hep-ph]].
- [217] R. Aaij *et al.* [LHCb], “Measurement of CP -Averaged Observables in the $B^0 \rightarrow K^{*0} \mu^+ \mu^-$ Decay,” *Phys. Rev. Lett.* **125** (2020) no.1, 011802 doi:10.1103/PhysRevLett.125.011802 [arXiv:2003.04831 [hep-ex]].
- [218] M. Algueró, A. Crivellin, S. Descotes-Genon, J. Matias and M. Novoa-Brunet, “A new B -flavour anomaly in $B_{d,s} \rightarrow K^{*0} \bar{K}^{*0}$: anatomy and interpretation,” *JHEP* **04** (2021), 066 doi:10.1007/JHEP04(2021)066 [arXiv:2011.07867 [hep-ph]].
- [219] M. Algueró, P. A. Cartelle, A. M. Marshall, P. Masjuan, J. Matias, M. A. McCann, M. Patel, K. A. Petridis and M. Smith, “A complete description of P- and S-wave contributions to the $B^0 \rightarrow K^+ \pi^- \ell^+ \ell^-$ decay,” [arXiv:2107.05301 [hep-ph]].
- [220] M. Algueró, B. Capdevila, S. Descotes-Genon, P. Masjuan and J. Matias, “What R_K and Q_5 can tell us about New Physics in $b \rightarrow s \ell \ell$ transitions?,” *JHEP* **07** (2019), 096 doi:10.1007/JHEP07(2019)096 [arXiv:1902.04900 [hep-ph]].
- [221] R. Aaij *et al.* [LHCb], “Tests of lepton universality using $B^0 \rightarrow K_S^0 l^+ l^-$ and $B^+ \rightarrow K^{*+} \ell^+ \ell^-$ decays,” [arXiv:2110.09501 [hep-ex]].